


GEOLOGI FOR SAMFUNNET

GEOLOGY FOR SOCIETY



Report no.: 2008.074		ISSN 0800-3416	Grading: Confidential to 31.12.10
Title: Lithochemical investigations of potential apatite resources in the Misværdal and Hopsfjellet ultramafic massifs, northern Norway			
Authors: Peter M. Ihlen		Client: Yara International ASA	
County: Nordland		Commune: Bodø	
Map-sheet name (M=1:250.000) Bodø, Sulitjelma, Mo i Rana		Map-sheet no. and -name (M=1:50.000) 2029-2 Misvær, 2029-4 Bodø, Valnesfjord 2029-4	
Deposit name and grid-reference: See Appendix 4		Number of pages: 57	Price (NOK): 215,-
Fieldwork carried out: 8.-26.07.2008	Date of report: 31.12.08	Project no.: 326600	Person responsible:  Rognvald Boyd

Executive summary:

Background:

The Misværdal massif, with a surface extension of ca. 8 km², is situated near the sea; about 130 km from Glomfjord by boat (Figures 1-2). Its apatite potential was recognized in 2007 by Nordland Mineral, an organisation established and financed by the county administration in Nordland and collaborating with the Geological Survey of Norway (NGU). Yara International ASA was contacted in 2008 for economic support and agreed to finance lithochemical investigations in collaboration with NGU.

Target:

The ultimate target for the investigations was to define a potential open-pit area exceeding 200 000 m² and containing rocks with an average grade of minimum 6 % P₂O₅.

Investigations:

112 rock samples were collected from the different rock types constituting the Misværdal ultramafic massif. It was planned to be covered by 133 samples in a 250 m quadratic grid. However, the sampling points of the grid had to be adjusted in the course of the sampling due to extensive overburden and deep weathering.

Results:

The Misværdal pyroxenite massif is rich in phosphorus with an average grade for all the sampled ultramafic rocks (106) of 2.1 % P₂O₅ or 5 % calculated apatite (Figures 25-26). 9 % of them give an average of 6.1 % P₂O₅ (10 samples >5.0 % P₂O₅) with a maximum of 6.6 % P₂O₅ (~15.5 % apatite, Figure 27). The high-grade samples are nearly invariably derived from coarse-grained ultramafic units, emphasizing a potential lithological control of the apatite enrichment (Figure 28). 4 potential linear zones of coarse-grained rocks can speculatively be defined, each with thicknesses in the range 50-200 m and covering areas of 180 000-250 000 m² (Figure 29). Their average grades are difficult to estimate due to varying P₂O₅ contents, even over relatively short distances.

Increased knowledge about magmatic apatite deposits gained through the project has also lead to the recognition of other potential target areas both in the Misvær region (Figure 30) and elsewhere in the Caledonides of Norway (Figure 9).

Recommendations:

In view of the ultimate target and the limited resources invested in the project the results are promising and warrant follow-up work. This is also supported by the petrographical similarities between the apatite-rich ultramafic rocks of the Misværdal massif and those hosting mineable copper-sulphide and apatite ores in the Palaborwa alkaline complex of South Africa. The next step is to determine more accurately the extent and average grades of the individual coarse-grained units by mapping and sampling of those exceeding 50 m in thickness. Dense sampling can be conducted by portable core-driller in profiles across well-exposed parts of the units and by hammer in other small outcrops between profiles. However, it is recommended that this work is not conducted before the contents of potential contaminants (chlorine, arsenic) and economic elements (rare earth oxides) in the apatite have been determined by microprobe analyses. Total analytical and sampling costs are estimated to NOK 350 000.

Keywords: Lithochemistry	Clinopyroxenite	Apatite
Alkaline igneous complex	Geology	Alkali metasomatism
Carbonatite dykes	Syenite dykes	P ₂ O ₅ analyses

CONTENTS

1. INTRODUCTION	6
2. SAMPLING PROCEDURE AND ANALYSES	6
3. GEOLOGICAL OUTLINE	10
3.1 <i>The Misværdal massif</i>	12
3.1.1 Age	12
3.1.2 Deformation	12
3.1.3 The main lithologies	17
3.1.4 Alkali metasomatism-fenitisation	20
3.1.5 Microscope examinations of the apatite-bearing rocks	20
3.2 <i>The Hopsfjellet massif</i>	26
4. ANALYTICAL RESULTS	26
4.1 <i>Misværdal</i>	26
4.2 <i>Hopsfjellet</i>	31
5. ASSESSMENT OF THE APATITE POTENTIAL.....	33
6. AEROMAGNETIC SIGNATURES	35
7. CONCLUSIONS.....	36
8. RECOMMENDATIONS	37
9. REFERENCES.....	37

FIGURES

Figure 1. <i>Geological map of Nordland showing the location of Misværdal and Hopsfjellet ultramafic massifs in relation to Bodø and Glomfjord.</i>	7
Figure 2. <i>The geological setting of the Misværdal and Hopsfjellet ultramafic massifs. Map compiled from Gjelle (1988), Gustavson and Gjelle (1991), Gustavson and Blystad (1995), and Gustavson (1996).</i>	8
Figure 3. <i>Sector of topographic map sheet Misvær (1:50 000, M711, 2029-2 with UTM grid) showing the outline of the Misværdal massif (pale purple, Solli et al. 1992) with planned sampling points in a 250 m quadratic grid.</i>	9
Figure 4. <i>Image showing the view from the top of Flågan westwards through the massif towards the main road (R812) and the Kårbøl farms.</i>	9
Figure 5. <i>Road cut along Kårbøl road at sample locality 47661 (see Figure 6) showing pre-glacial deep weathering in the upper 2 metres of the section.</i>	10
Figure 6. <i>Outline of northern and southern pyroxenite bodies with sample localities and numbers.</i> ...	11

Figure 7. Geological map of the Misværdal pyroxenite massif taken from Solli et al. (1992).	13
Figure 8. Map showing the distribution of sampled lithologies together with observed zones of coarse-grained pyroxenites and the strike direction of wall-rock rafts in the pyroxenites.	14
Figure 9. Simplified map of the Scandinavian Caledonides showing the distribution of carbonatite-bearing alkaline complexes of Late Neoproterozoic age.	15
Figure 10. Image looking north along the foliation of feldspar-veined medium-grained pyroxenites.	15
Figure 11. Shear zone in pyroxenites on the mountain plateau between sampling points SKM 34 and 35.	16
Figure 12. Hinge zone of open fold defined by carbonatite dyke in medium-grained biotite-altered pyroxenites.	16
Figure 13. Dark grey, coarse-grained and pervasively biotite-altered pyroxenite truncating nearly unaltered medium-grained pyroxenites.	18
Figure 14. Coarse-grained biotite "gabbro" with needle-shaped to irregular intergranular aggregates of apatite.	18
Figure 15. Pale pinkish grey feldspathic carbonatite dyke with cm sized pyroxene crystals that also form dark aggregates in the surrounding weakly foliated medium-grained biotite-pyroxenite.	19
Figure 16. Globulite composed of 5 mm felsic globules in a pyroxenite matrix (upper left corner) that is cut by irregular felsic dykes with small globulite lenses.	19
Figure 17. Irregular network of light grey calcite-feldspar veins coalescing into thicker carbonatite lenses (0.5m, upper right corner) in weakly biotite-altered medium-grained pyroxenites.	21
Figure 18. Medium-grained pyroxenite with coarse-grained clinopyroxene segregations with interstitial aggregates of feldspar and some calcite.	21
Figure 19. Coarse-grained augite (Cpx) intergrown with prismatic aggregates of apatite (Ap). Brownish metasomatic allanite (Al) and light bluish-green metamorphic actinolite (Act) replace the augite grains and corrode the apatite.	23
Figure 20. Segment of large intergranular aggregate of apatite (Ap) intergrown with brown slightly deformed biotite (Bi), augite (Cpx) partly replaced by actinolite (Act) and black opaques (mainly pyrite).	23
Figure 21. Apatite crystals (Ap) occurring intimately intergrown with biotite (Bi) and augite (Cpx), all of them showing incipient replacement by actinolite (Act) and aggregates of sodic plagioclase (Pl), calcite (Cc) and allanite (Al).	24
Figure 22. Interstitial grains and aggregates of apatite (Ap) in biotite-poor pyroxenite composed of light green augite (Cpx).	24
Figure 23. Medium-grained pyroxenite composed of augite (Cpx) with interstitial grains and aggregates of apatite (Ap), metasomatic green biotite (Bio) and opaques (black, pyrite and chalcopyrite).	25

Figure 24. <i>Elongated aggregates and disseminated single grains of apatite (Ap) in weakly deformed brownish green biotite (Bi) and a formerly augite crystal pseudomorphically replaced by fibrous aggregates of actinolite (Act).</i>	25
Figure 25. <i>Map showing the distribution of P₂O₅ in the Misværdal pyroxenite massif. All samples of alkaline rocks collected during the period 2006-2008 are shown.</i>	28
Figure 26. <i>Map showing the distribution of calculated apatite contents in the Misværdal pyroxenite massif. All samples of alkaline rocks collected during the period 2006-2008 are shown.</i>	29
Figure 27. <i>Histograms showing number (N) of samples within given 1 % intervals of weight % P₂O₅. Medium-grained rocks in red (top) compared to coarse-grained rocks in grey (top) that are shown separately in dark blue (bottom).</i>	30
Figure 28. <i>Map showing the distribution of P₂O₅ in the Misværdal pyroxenite massif in relation to type of alkaline rock in the analysed sample. All samples of alkaline rocks collected during the period 2006-2008 are shown.</i>	31
Figure 29. <i>Map showing the location of potential apatite-rich zones (red) in the Misværdal massif that deserve follow-up work.</i>	34
Figure 30. <i>Aeromagnetic anomaly map showing the location of mafic-ultramafic bodies in the Misvær area. Map compiled from magnetic data in the NGU geophysical database and bedrock map Misvær, 1:50000 (Solli et al. 1992).</i>	35

TABLES

Table 1. <i>Mineral assemblages related to the different petrogenetic stages of the Misværdal massif.</i> ..	20
Table 2. <i>Statistical data for 107 analyses of P₂O₅ in mafic-ultramafic rocks of the Misværdal massif, excluding analyses of samples from globulites, syenites and wall rocks (gneisses, marbles, soapstones and granitoids).</i>	27
Table 3. <i>Statistical data of P₂O₅ contents of analysed rocks sampled in the period 2006-2008.</i>	32

APPENDIX

Appendix 1. <i>Sample weight in kilogram and analytical values for P₂O₅ in weight % listed in numerical sample order for the period 2006-2008.</i>	39
Appendix 2. <i>Analytical values for P₂O₅ in weight % listed in order of decreasing values.</i>	43
Appendix 3. <i>Analytical values for P₂O₅ in weight % grouped according to lithological types and then listed in order of decreasing values.</i>	47
Appendix 4. <i>Sample list showing the coordinates of the sampling points and petrographic description of the collected samples together with their lithological code shown in Appendix 5.</i>	51
Appendix 5. <i>Table showing the different abbreviations or lithological codes for the sampled rocks shown in Appendix 1-4 together with transformation factors used in the calculation of apatite contents and grain-size terminology used in the text.</i>	57

1. INTRODUCTION

The investigations were conducted in accordance with the project proposal given by Ihlen (2008) and a contract for the collaboration between Yara International ASA (Yara) and the Geological survey of Norway (NGU). The aim of the work was to define potential apatite resources within the Misværdal ultramafic massif (8 km²) and to do comparative studies of the Hopsfjellet ultramafic massif (17 km²) which has no known apatite-rich rocks. Both are situated near the sea in the Salten region of Nordland (Figures 1-2), a short distance from Yara's plant in Glomfjord (100-130 km by boat). The ultimate goal is to define an open pit area of minimum 200 000 m² containing rocks with an average grade exceeding 6 % P₂O₅. The investigations were based on lithochemical sampling followed by whole rock analyses of P₂O₅, and total analyses of major and trace elements in selected samples. The analyses were conducted by Acme Analytical Laboratories Ltd in Vancouver, BC, Canada. The sampling was carried out in the period 8-26th July 2008 by the Geological Survey of Norway (NGU), i.e. by senior geologist Peter M. Ihlen assisted by engineer Leif Furuhaug. 117 samples were shipped for analyses at August 2nd, and the analytical results were received from Acme Laboratories on October 12th.

2. SAMPLING PROCEDURE AND ANALYSES

Grab samples were collected with a hammer from rocks in outcrops and road cuts. In the Misværdal case some of the small outcrops may represent large boulders (see Figure 6). In order to determine the potential geological control of the distribution of phosphorus the dominant lithology was collected at each sampling point and no attempt was made to make an average of the different lithologies in outcrops containing several rock types. The geology at the sampling points was registered, but only briefly inspected on the course to next locality. Proper geological bedrock mapping has therefore **not been** conducted in any part of the two massifs.

The size of the collected samples (1-3 kg) depends largely on number of samples to be carried in the pack sack at the end of the day and on the distance to the nearest road in the case of the Misværdal massif. Fist-sized reference samples were removed and stored at NGU before the rest were shipped to Canada for analyses. The total weight of the analysed samples is given in Appendix 1 together with the analytical results. Sample descriptions are found in Appendix 4 together with the UTM coordinates of the sampling points, whereas Appendix 5 contains lithological codes used in Appendixes 1-3 together with apatite calculation coefficients and grain size classifications.

The rocks of the Hopsfjellet massif were inspected along road R80 where they are beautifully exposed on the northern shore of Hopen bay (Figure 2). Only 5 samples were collected since the geological field relationships strongly indicated that the mafic-ultramafic rocks represent meta-volcanites with no apparent apatite potential. The Misværdal massif was originally planned to be covered by 133 samples in a 250 m quadratic grid (Figure 3). The low density of outcrops in areas with Quaternary cover, together with the effect of pre-glacial deep weathering in a number of outcrops made it difficult to follow this sampling procedure precisely (Figures 4-5).

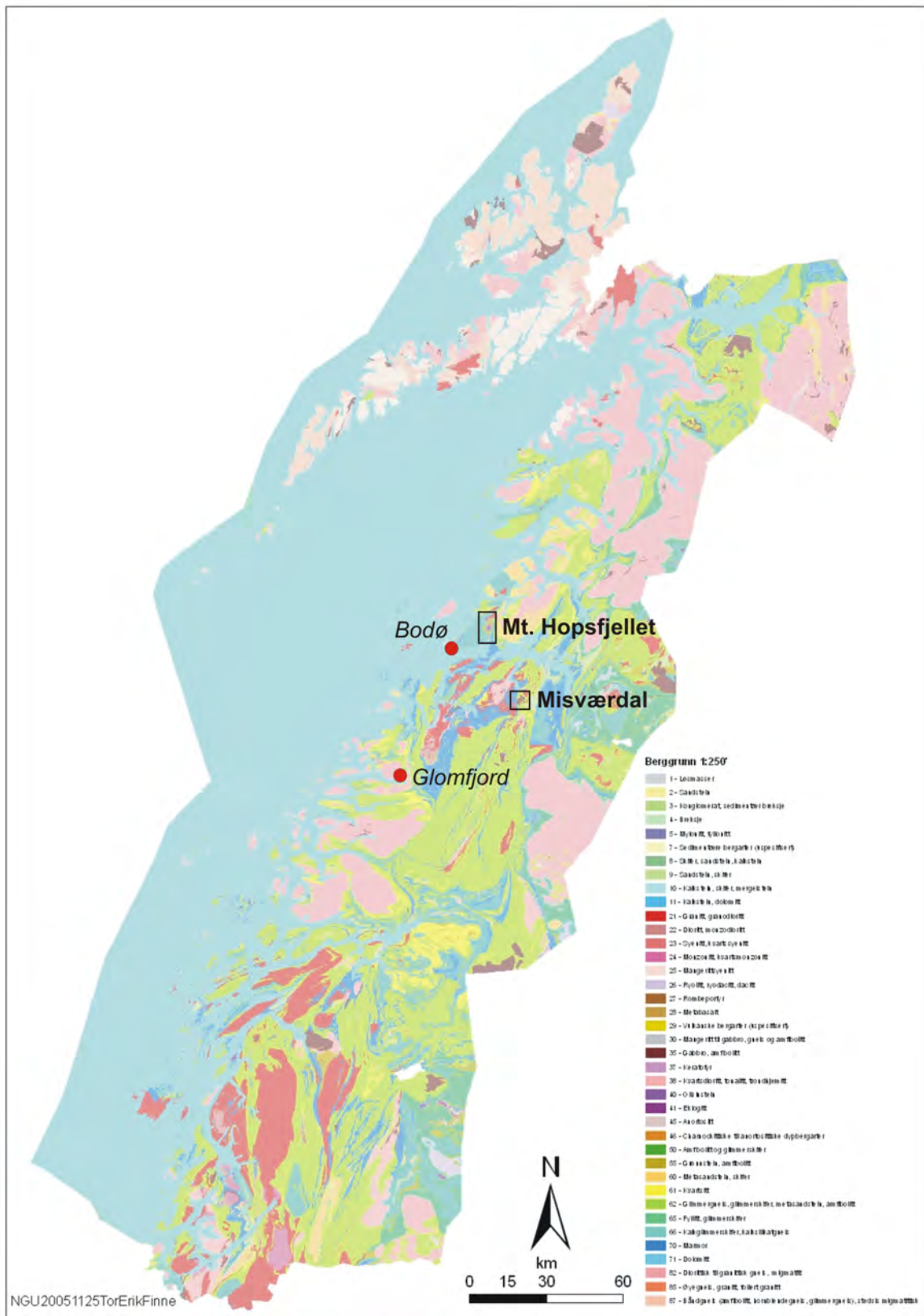


Figure 1. Geological map of Nordland showing the location of Misværdal and Hopsfjellet ultramafic massifs in relation to Bodø and Glomfjord.

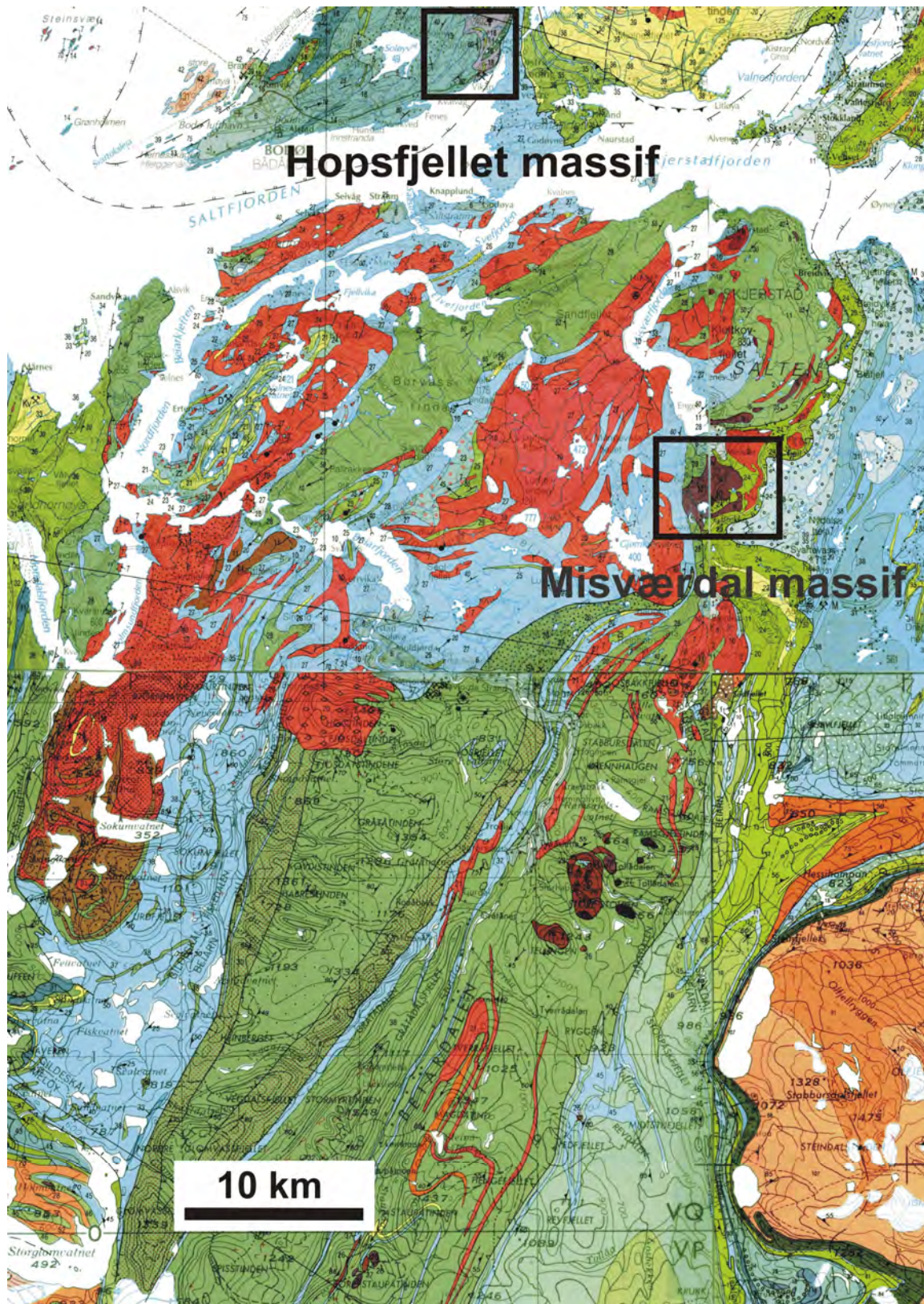


Figure 2. The geological setting of the Misværdaal and Hopsfjellet ultramafic massifs (violet, brown, purple). Map compiled from Gjelle (1988), Gustavson and Gjelle (1991), Gustavson and Blystad (1995), and Gustavson (1996). Red and brown dotted = calc-alkaline granitoids (Late Ordovician); Orange = alkaline granitoids; Bluish = calcite and dolomite marbles including carbonate conglomerates; Greenish to bluish green = mica and calc-silicate schists/gneisses; Yellowish = quartzites; Pale brown to beige (in the east) = Palaeoproterozoic orthogneisses (basement).

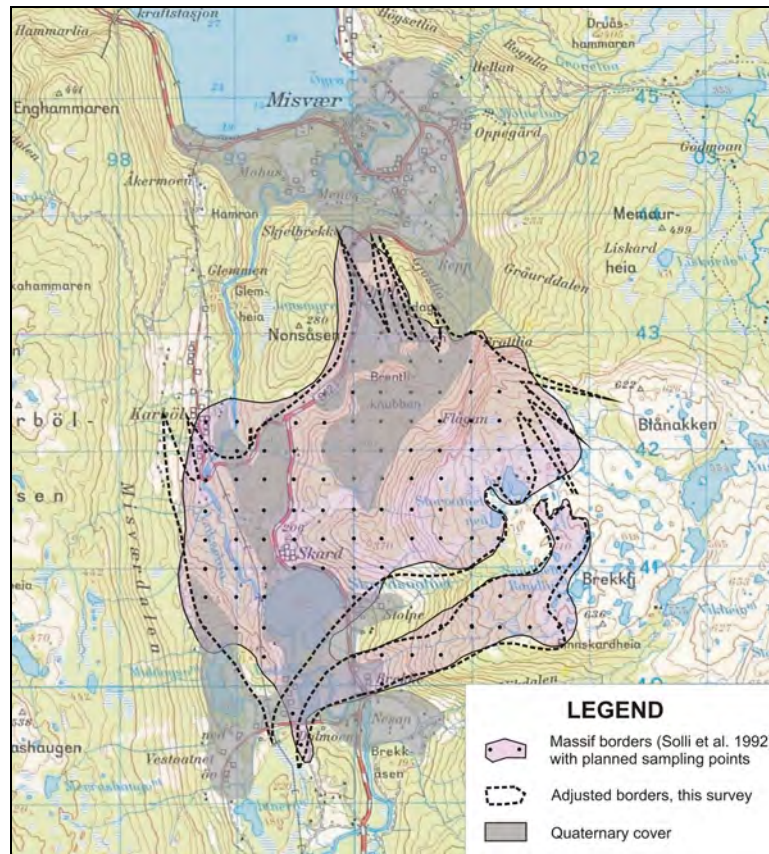


Figure 3. Sector of topographic map sheet Misvær (1:50 000, M711, 2029-2 with UTM grid) showing the outline of the Misværdal massif (pale purple, Solli et al. 1992) with planned sampling points in a 250 m quadratic grid. The dashed line gives the adjusted outline of the southern and northern pyroxenite bodies. Grey shading represents Quaternary deposits and pre-glacial deep weathering.



Figure 4. Image showing the view from the top of Flågan westwards through the massif towards the main road (R812) and the Kårbøl farms. The green, densely forested area south of Brentliknubben in the lower half of the picture contains very few outcrops.



Figure 5. Road cut along Kårbøl road at sample locality 47661 (see Figure 6) showing pre-glacial deep weathering in the upper 2 metres of the section composed of medium-grained pyroxenites with light grey syenite dykes.

In addition, some outcrops (often sub-vertical cliffs) have too smooth surfaces (polished by glaciers) to be sampled by hammer. The end result is 112 samples with inter-sample distances of 150-500 m as depicted in Figure 6. Localities with two densely spaced samples are due to the presence of two contrasting lithologies, in most cases ultramafics and carbonate rocks (potential carbonatites). The sampling in Misværdal was time consuming primarily due to dense vegetation of birch trees and 1-1.5 m high herbs and ferns that were difficult to penetrate. Secondly, many of the outcrops represent nearly inaccessible sub-vertical cliffs at the top of very steep, scree-covered and strongly vegetated slopes (e.g. SKM 40 and 41). The samples were crushed, pulverized and analyzed by Acme. All the samples were analyzed for P_2O_5 by ICP-ES (Analytical procedure 4A) on 0.1 gram split of the pulverized material (200 gram). The analytical results are given in Appendixes 1-3. In addition, 20 samples of the main lithologies of the Misværdal massif were analyzed for major and trace elements by ICP-MS and ICP-ES (4A+4B+1DX) and 7 samples of carbonate rocks by ICP-ES (1E) to test their origin as carbonatites (Sr).

3. GEOLOGICAL OUTLINE

This part of the report is solely based on observations in the field aided by the use of a hand lens (10x). The terminology used for the lithologies must therefore be regarded as preliminary field terms. Both of the investigated massifs form an integral part of the Uppermost Allochthon of the Scandinavian Caledonides (see Figure 9).

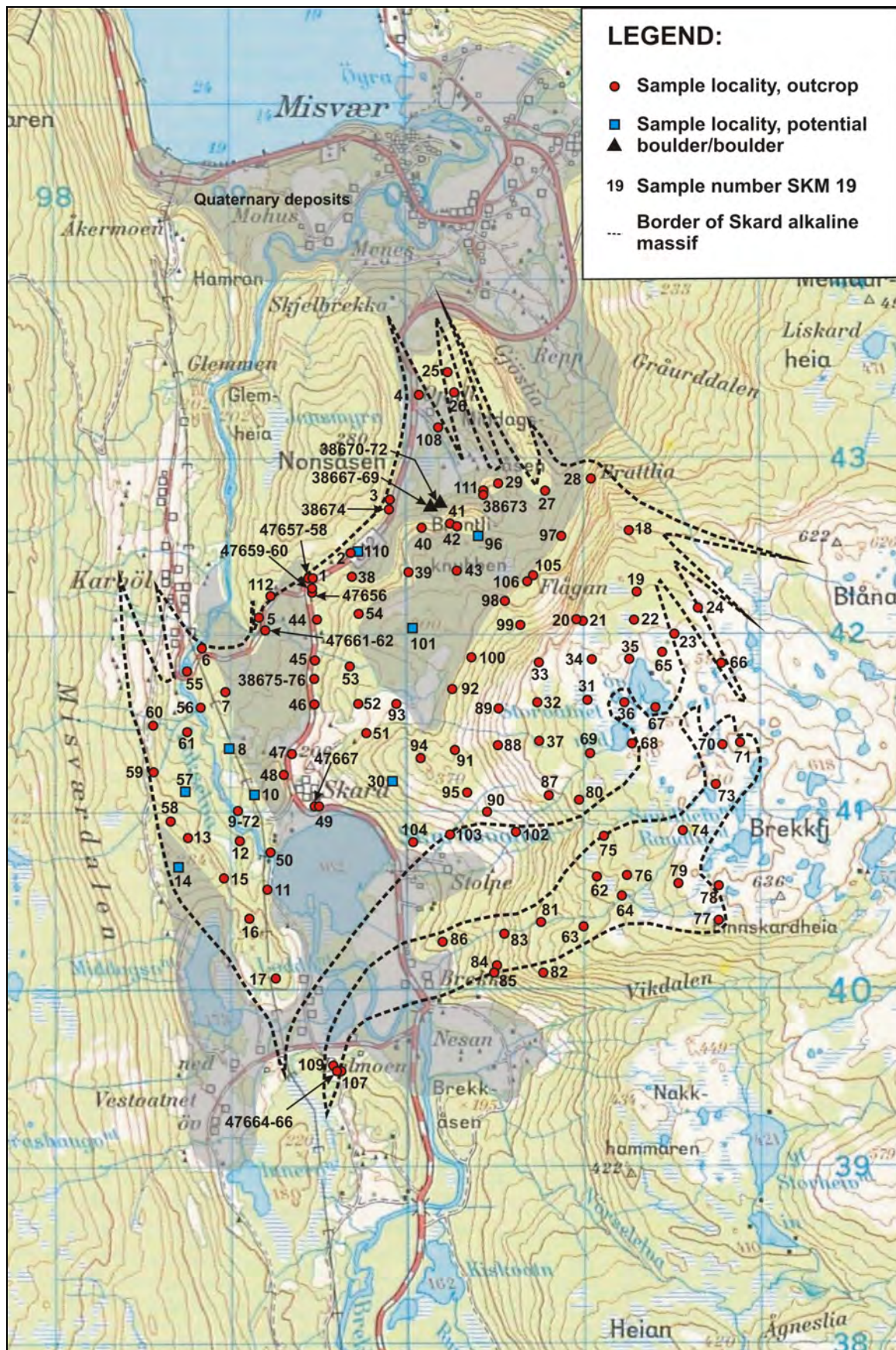


Figure 6. Outline of northern and southern pyroxenite bodies with sample localities and numbers. Five digit numbers starting with 47 sampled for Nordland Mineral in 2006 and those starting with 38 in 2007.

3.1 The Misværdal massif

The Misværdal massif, covering an area of about 8 km², was first discovered by Farrow (1974) who recognized its alkaline chemistry including the enrichment of phosphorus (max. 5.2 % P₂O₅). One of the reasons that the massif has stayed unnoticed for years is that it, in contrast to other alkaline complexes, is composed of rocks low in ferromagnetic minerals like Fe-Ti oxides. Thus it is only represented by a weak, but distinct magnetic anomaly on aeromagnetic maps.

The massif appears to comprise two separate pyroxenite bodies (northern, 6.5 km² and southern, 1.5 km²) (Figure 6) that intrude mainly mica schists, micaceous migmatitic gneisses and marbles of sedimentary origin. The pyroxenites locally contain rafts of these wall rocks, as well as of gneisses with lenses of soapstone. In addition, the pyroxenites are found as inclusions in some of the outcropping granodiorites and quartz diorites inside the massif. These granitoids are related to the emplacement of Late Ordovician calc-alkaline granitic intrusions in the surrounding country rocks (Tørudbakken and Brattli 1985; Figures 7-8). The regular outline of the massif shown in published maps (e.g. *Solli et al. 1992*) is a simplification (Figure 7). Observations made during the sampling strongly suggest more irregular boundaries with several apophyses cutting the surrounding meta-sedimentary rocks along their penetrative N-NW-trending foliation (Figure 3). Aeromagnetic maps give indications that the massif continues at depth towards the west.

3.1.1 Age

The massif truncates the thrust zone separating the Beiarn and Rödingsfjell Nappe Complexes according to the regional geological bedrock maps (Figures 2 and 7). Thus the massif post-dates the Late Cambrian -Early Ordovician amalgamation of these nappes (Finnmarkian/Taconian orogeny), but pre-dates the Late Ordovician calc-alkaline granitoid intrusions and the Late Silurian continent-continent collision (Scandian orogeny) when the Caledonides ultimately were formed. However, the location of this thrust is very speculative since there appears to be no particular lithological or metamorphic break across it. If the thrust zone is, instead, located east of the massif, as shown in Figure 7, the massif could be late Neoproterozoic in age and similar in age to other carbonatite-bearing alkaline complexes in Scandinavia (Figure 9).

3.1.2 Deformation

The pyroxenites are generally only weakly deformed with a faint to distinct semi-penetrative foliation in the finer grained and biotite-bearing varieties (see Figure 18). Penetrative foliation, affecting all of the rocks in the two pyroxenite bodies, is only developed along their margins and along thin shear zones in their interior (Figures 10-11). In addition, there are occasionally pygmatic folded dykes and bands with pinch and swell structure. There are no indications of large-scale tight folds, although indications of open meso-scale folds are seen locally (Figure 12). The metamorphic overprint appears to be weak and includes the formation of biotite-coated foliation planes, and actinolite- and epidote-filled fractures enveloped by mineral alteration assemblages typical of greenschist facies (Figures 12).

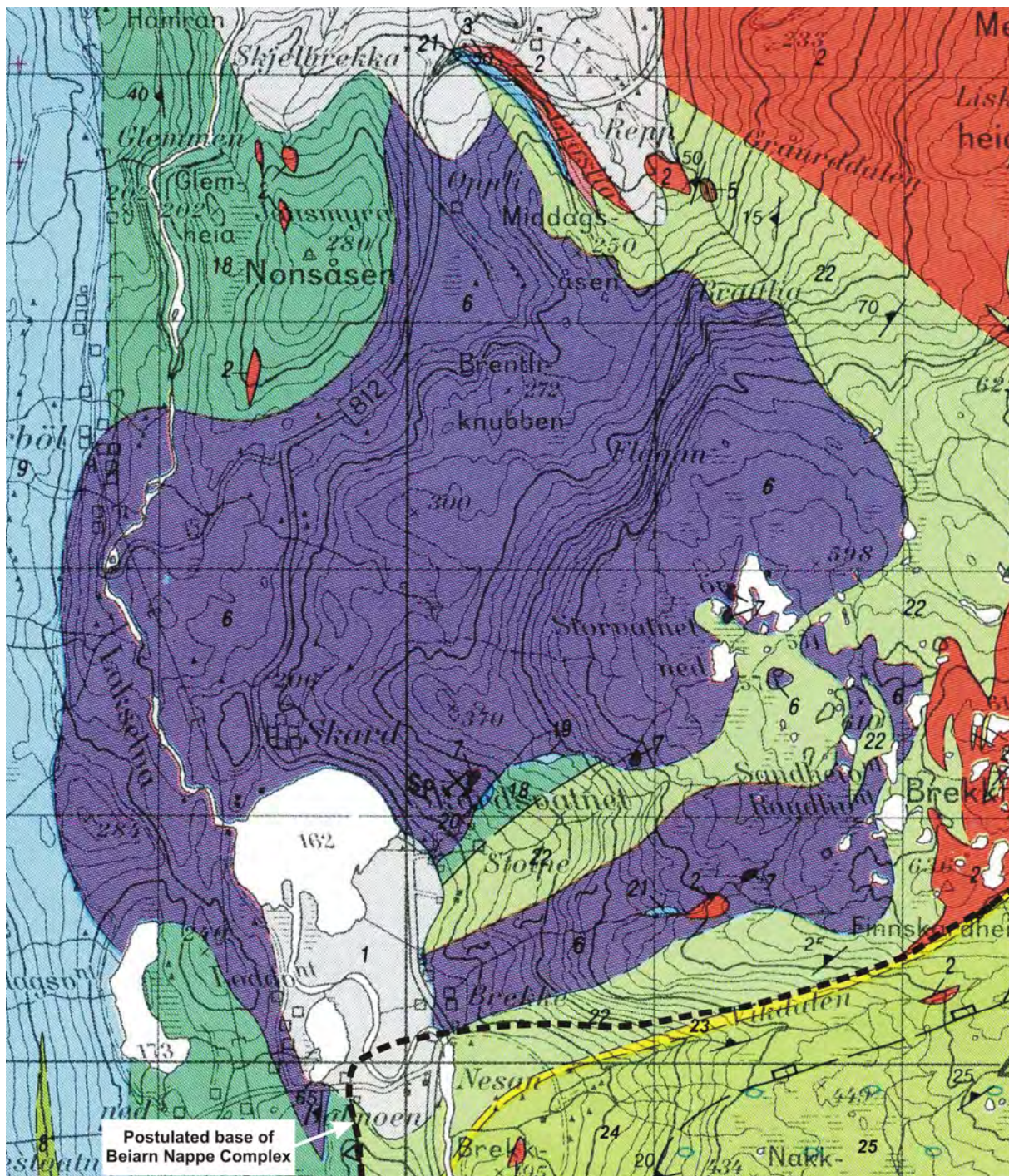


Figure 7. Geological map of the Misværdal pyroxenite massif taken from Solli et al. (1992). 1=Quaternary deposits, 2=Granites and granodiorites, 3=Tonalites and quartz diorites, 5=Metagabbros, 6=Pyroxenites, 7=Soapstones, Beiarfjell Nappe Complex: 8=Staurolite schists, 9=Calcite marbles, 18=Micaceous gneisses, partly migmatitic, Rödingsfjell Nappe Complex: 22=Garnetiferous mica schists, 23=Quartzite, 24= Garnetiferous quartz-mica schists, Köli Nappe Complex: 25=Conglomeratic calcareous mica schists.

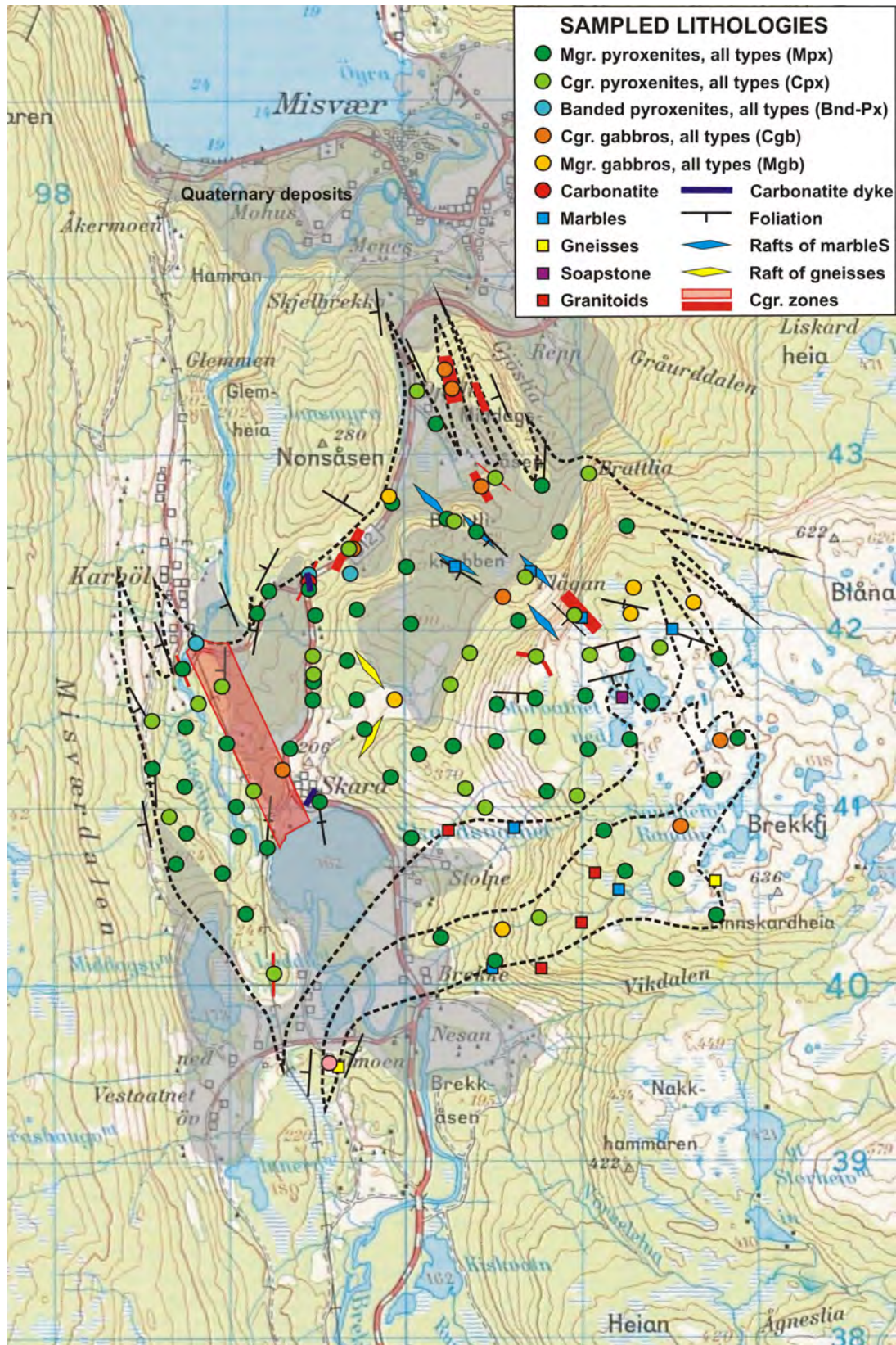


Figure 8. Map showing the distribution of sampled lithologies together with observed zones of coarse-grained pyroxenites and the strike direction of wall-rock rafts in the pyroxenites.

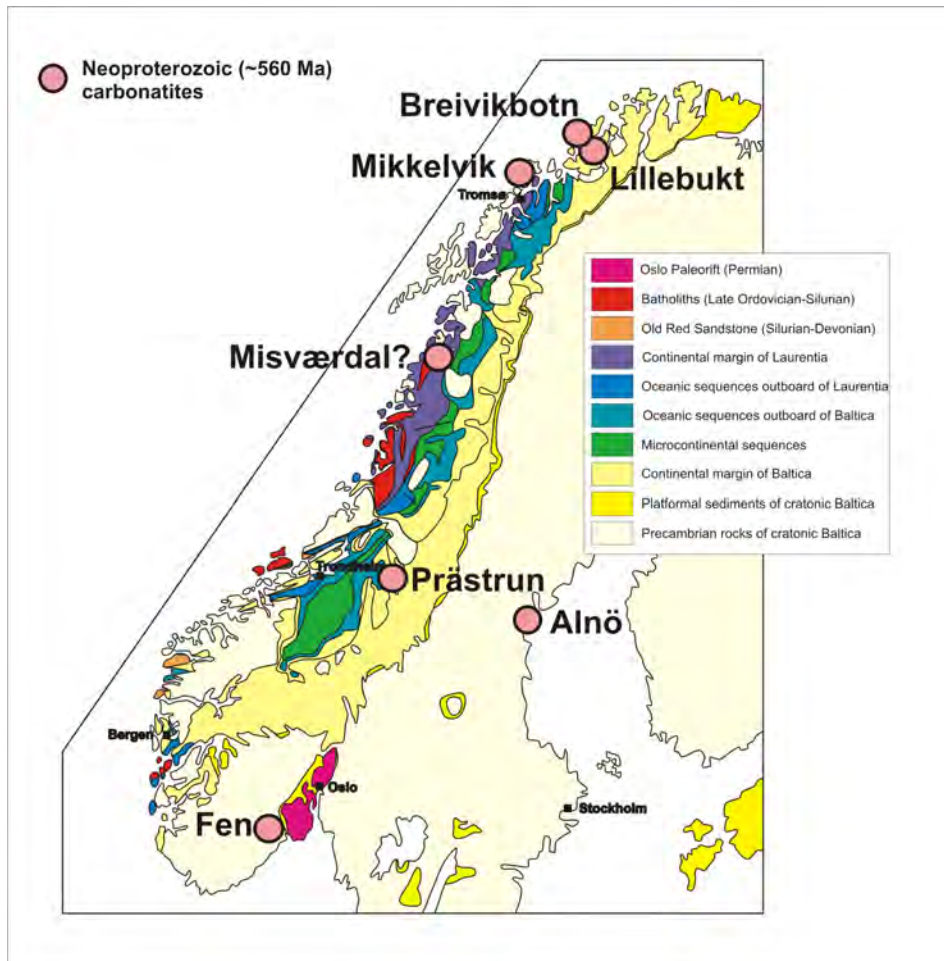


Figure 9. Simplified map of the Scandinavian Caledonides showing the distribution of carbonatite-bearing alkaline complexes of Late Neoproterozoic age.



Figure 10. Image looking north along the foliation of feldspar veined medium-grained pyroxenites. Outcrop in river bed about 100 m west of sampling point SKM 60.



Figure 11. *Shear zone in pyroxenites on the mountain plateau between sampling points SKM 34 and 35. Strike and dip are N63°E and 70° SE, respectively. Notice the low density of outcrops even above the tree line as seen in the background towards the west.*



Figure 12. *Hinge zone of open fold defined by carbonatite dyke in medium-grained biotite-altered pyroxenites. The dark envelopes of the dykes represent pervasive biotitisation. The light hairline veins along axial plane fractures are composed predominantly of calcite and actinolite. Sampling point 47660 at the junction between R812 and the Kårbøl road.*

3.1.3 The main lithologies

Both pyroxenite bodies are composed predominantly of light to dark green medium-grained (1-3 mm) pyroxenites (MPx, Figure 13). Their colours are dependent on the proportions of clinopyroxene, biotite, hornblende, feldspar and actinolite. They appear to be devoid of Fe-Ti oxides, although the carbonatite dykes locally contain abundant fine-grained magnetite. In the northern body the MPx commonly contains units of coarse- (3-10 mm) to very coarse-grained (10-30 mm) varieties (CPx) that show thicknesses from 0.1 m to more than 50 m. The lack of extensive exposures and the large distances between them makes it nearly impossible to define the true thicknesses and the strike extension of the CPx units that contain the highest concentrations of phosphorus (Figure 8). They appear mostly to have S to SE strikes with 40°-80° W-SW dips. The MPx appears to be more resistant to weathering than the CPx and is possibly overrepresented in the outcrops even in the best exposed areas above the tree line (c.550 m.a.s.l.) at the Storvatn plateau (Figure 11).

The CPx units can be separated into common pyroxenites and feldspathic pyroxenites (ca. 5-10 % fsp, Fsp-CPx) with further subdivision according to their contents of biotite (Bio-CPx, FspBio-CPx). Some of the CPx are termed CGb due to their gabbroic appearance caused by abundant light gray and coarse acicular crystals and interstitial aggregates of apatite (Figure 14), as well as aggregates of alkali feldspar and plagioclase. Due to the difficulty in determining the relative amounts of the different types of feldspars in the field, as well as apatite, some of the CGb would certainly have been classified as Fsp-CPx or CPx, if microscope examinations were performed. However, true gabbros are encountered in the massif, but mainly as small, medium-grained bodies with high contents of evenly distributed sub-ophitic calcic plagioclase. The CPx units containing magmatic biotite (see chapter 3.1.4) probably crystallised from highly potassic volatile-rich melts. Formation of such melts by fractionation of the MPx magma during crystallisation is suggested by the local presence of thin, alternating bands of MPx and CPx resembling igneous layering and the development of Cpx patches in the MPx. However, the apophyses occurring in the gneisses at Middagsåsen consist solely of CGb similar to that shown in Figure 14 with small domains of Cpx. This may indicate that the CPx and associated gabbros represents residual melts that intruded the MPx massif and its wall rocks during a separate magmatic event. Other magmatic events include late intrusions of scattered thin lenses and veins of carbonatites and dm to meter thick linear dykes of syenite (SKM 1 and 72). The carbonatites show variable grain sizes and contents of calcite, coarse crystals of clinopyroxene, up to 5 mm crystals of dull greenish grey apatite, as well as pale pinkish fine- to medium-grained alkali feldspar and accessory barite (Figures 12 and 15). The syenites are composed dominantly of very coarse-grained (10-30 mm) bluish grey alkali feldspar intergrown with minor quartz. Other rocks sampled include globulites or orbicular rocks that occur at the southwestern end of both bodies (Figure 16). They are caused by mingling of the ultramafic melt with felsic melts either caused by partial melting of the gneisses along the contact or most likely by liquid immiscibility during magma fractionation.



Figure 13. Dark grey, coarse-grained and pervasively biotite-altered pyroxenite truncating nearly unaltered medium-grained pyroxenites (lighter greyish green). The 1 m thick tongue-like biotite-rich body is seen in the left and central part of the image. Light grey veins represent calcite-feldspar veins. Road-cut north of the lake, Skardsvatn at sampling point SKM 49.



Figure 14. Coarse-grained biotite "gabbro" with needle-shaped to irregular intergranular aggregates of apatite. Picture from locality SKM 111 where the analyses return 0.5 % Na_2O , 4.4 % K_2O and 5.9 % P_2O_5 . The diameter of the coin is 2.5 cm.



Figure 15. *Pale pinkish grey feldspathic carbonatite dyke with cm sized pyroxene crystals that also form dark aggregates in the surrounding weakly foliated medium-grained biotite-pyroxenite. Coin as scale is 2 cm in diameter. Locality 20 m south of the carbonatite dyke in Figure 12.*



Figure 16. *Globulite composed of 5 mm felsic globules in a pyroxenite matrix (upper left corner) that is cut by irregular felsic dykes with small globulite lenses. Notice the weakly developed foliation. The diameter of the coin is 2.5 cm. Outcrop about 150 m southwest of sampling point SKM 17 near the southwestern contact of the northern body.*

3.1.4 Alkali metasomatism-fenitisation

The pyroxenites frequently show fracture-bound to pervasive biotite alteration generating bio-MPx and bio-CPx with up to 90 % biotite. This type of alteration is especially abundant in areas with carbonatite lenses and veins that normally carry envelopes of pervasive biotite alteration of the pyroxenites (Figure 12). The biotitisation also occurs as an irregular infiltration of the ultramafic rocks (Figure 13) in conjunction with biotite-filled fractures in the medium-grained pyroxenites (MPx) and as intergranular aggregates in the coarse-grained varieties (CPx). Some pyroxenites have a banded structure that is caused both by biotitisation along systems of parallel fractures and by magmatic crystallisation. These are termed banded pyroxenites and include medium- and coarse-grained sub-types dependent on the dominant type in the sample (e.g. Bnd-CPx).

Networks of mm to cm wide alkali feldspar and/or carbonate veins (Fsp-Vnd-MPx) are also commonly encountered and some of them merge with wider lenses of feldspathic carbonatites (Figure 17). The individual feldspathic veins frequently occur associated with irregular infiltration of the adjacent wall rocks by medium-grained intergranular alkali feldspar and sodic plagioclase aggregates (Fsp-MPx), as well as by calcite. These minerals also fill the interstices between coarse crystals of clinopyroxene in patchy developed segregations in the MPx generating a gabbro-looking rock (Figure 18). These types of alteration that are widespread in both bodies most likely represent alkali metasomatism or fenitisation frequently occurring associated with the intrusion of residual volatile-rich (CO₂) melts in alkaline plutonic complexes; especially those containing carbonatite intrusions.

3.1.5 Microscope examinations of the apatite-bearing rocks

Microscope examination of the mafic-ultramafic lithologies reveals that their present mineral assemblages are caused by three different processes including magmatic crystallisation, late- to post-magmatic alkali metasomatism and subsequent metamorphism. The stable mineral assemblages formed during these stages are shown in Table 1.

Table 1. Mineral assemblages related to the different petrogenetic stages of the Misværdal massif. Colours of the minerals refer to their pleochroism under the microscope.

STAGE	MINERAL ASSEMBLAGE
Magmatic	Colourless to light greenish augitic pyroxene, brown to greenish brown biotite, apatite and locally dark green to brown sodic amphibole and accessory zircon
Late- to post-magmatic alkali metasomatism	Perthitic alkali feldspar, sodic plagioclase, green biotite, minor dark green sodic amphibole, and accessory allanite, calcite, titanite, zircon, pyrite, chalcopyrite, magnetite, ilmenite and pyrrhotite
Metamorphic	Green biotite, epidote, colourless to light green actinolitic amphibole, calcite, and minor quartz, chessboard albite, anthophyllite and chlorite



Figure 17. *Irregular network of light grey calcite-feldspar veins coalescing into thicker carbonatite lenses (0.5m, upper right corner) in weakly biotite-altered medium-grained pyroxenites. Strong biotite alteration in upper left corner. Same locality as Figure 13.*



Figure 18. *Medium-grained pyroxenite with coarse-grained clinopyroxene segregations with interstitial aggregates of feldspar and some calcite. These aggregates appear to merge with veins of similar mineralogy, some being affected by shearing (bottom right). The diameter of the coin is 2.5 cm. Same locality as Figure 17.*

Apatite is found in all of the mafic-ultramafic rocks in the Misværdal massif where its abundance ranges from a few scattered grains to abundant large aggregates of light greyish apatite grains. The subidiomorphic to idiomorphic apatite crystals are characterised by abundant fluid and melt inclusions (see Figure 20) that represent potential sinks of contaminating elements like chlorine and arsenic. Such contaminants can remain undetected during electron microprobe point analysis in contrast to the results from bulk chemical analyses of apatite concentrates that are recommended.

Although the individual apatite crystals are generally fine-grained, with grain sizes in the range 0.1-1.0 mm, they frequently cluster in monomineralic prismatic aggregates up to cm in length, especially in the CPx where the individual apatite crystals are up to 4 mm long (Figures 19-21).

The MPx is composed dominantly of granular aggregates of augitic clinopyroxene (0.2-4 mm) with variable contents of interstitial brown to brownish green pleochroic biotite (0.2-1.0 mm). The apatite occurs as dissemination of single grains (0.1-0.5 mm) and small aggregates rarely exceeding 1 mm. It occurs commonly as interstitial grains in the aggregates of magmatic augite and/or biotite aggregates (Figures 22-23), whereas prismatic to needle-shaped inclusions of apatite in augite, brown biotite and sodic amphibole are rather uncommon. All of these magmatic minerals are affected by subsequent metasomatic and metamorphic mineral reactions. The apatite grains become more xenomorphic and irregular when occurring within the fine-grained mineral aggregates formed subsequently to the magmatic stage (Figure 24). The alkali metasomatism comprises alteration of augite to sodic amphibole and formation of veinlets and aggregates of perthitic alkali feldspar and subordinate sodic plagioclase that replace augite and partly intergrown grains of apatite. The metamorphic overprint is recognised by pervasive alteration of augite and feldspar to aggregates of actinolite and epidote (<0.5 mm), as well as locally "chess board" albite, calcite, quartz and accessory chlorite. Epidote is often intergrown with or contains brown cores of early metasomatically formed allanite (orthite) that normally is enriched in light rare earth elements (LREE) including La and Ce. These minerals, with the exception of allanite, also fill hairline fractures often dominated by epidote and quartz+calcite. However, apatite appears to be absent from these veins and is also rarely found in mineral aggregates formed during the metasomatic and metamorphic stages.

A number of the apatite-bearing samples contain weakly disseminated to scattered grains of sulphides (0.01-0.5 mm). They appear to have precipitated during the metasomatic stage, occasionally together with magnetite that occurs as scattered grains (0.01-0.3 mm) in the silicates and/or forms thin rims around some of the pyrite grains. Those samples taken from outcrops with rusty patches on weathered surfaces are dominated by pyrite and/or pyrrhotite that occur together with accessory single grains of chalcopyrite in the silicates or contain small inclusions of it. In a few samples without rusty weathering, chalcopyrite is the dominant sulphide. Although the Cu-grade is generally low in the 26 multielement analyses of the mafic-ultramafic rocks (i.e. 5 samples yielding 0.01-0.02 % Cu and 0.1-0.5 % S), chalcopyrite should be tested as a potential byproduct in a high-tonnage apatite operation.

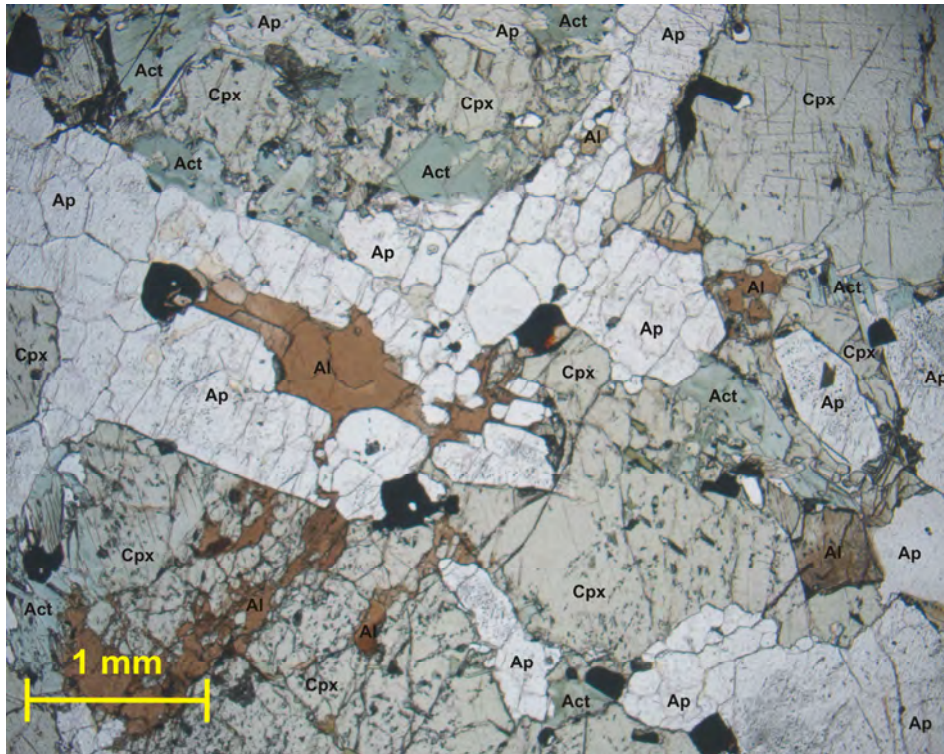


Figure 19. Coarse-grained augite (Cpx) intergrown with prismatic aggregates of apatite (Ap). Brownish metasomatic allanite (Al) and light bluish-green metamorphic actinolite (Act) replace the augite grains and corrode the apatite. The opaque minerals comprise mainly pyrite. Bio-CPx of sample SKM 111.

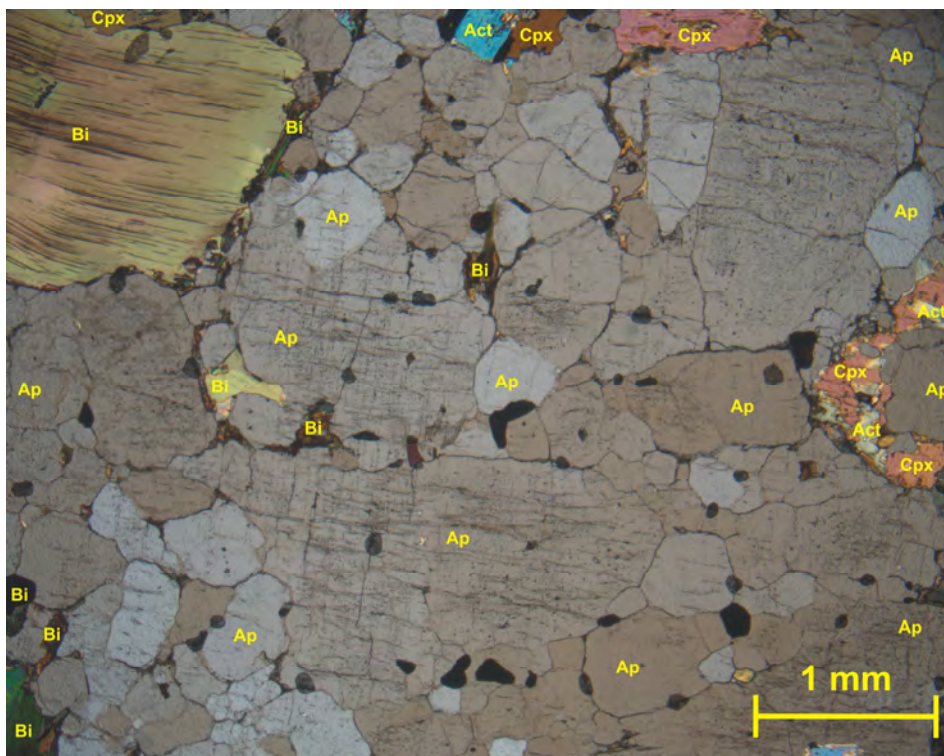


Figure 20. Segment of large intergranular aggregate of apatite (Ap) intergrown with brown slightly deformed biotite (Bi), augite (Cpx) partly replaced by actinolite (Act) and black opaques (mainly pyrite). The dust in the apatite grains represent fluid and melt inclusions. Partly crossed polars. Bio-CPx of sample SKM 111.

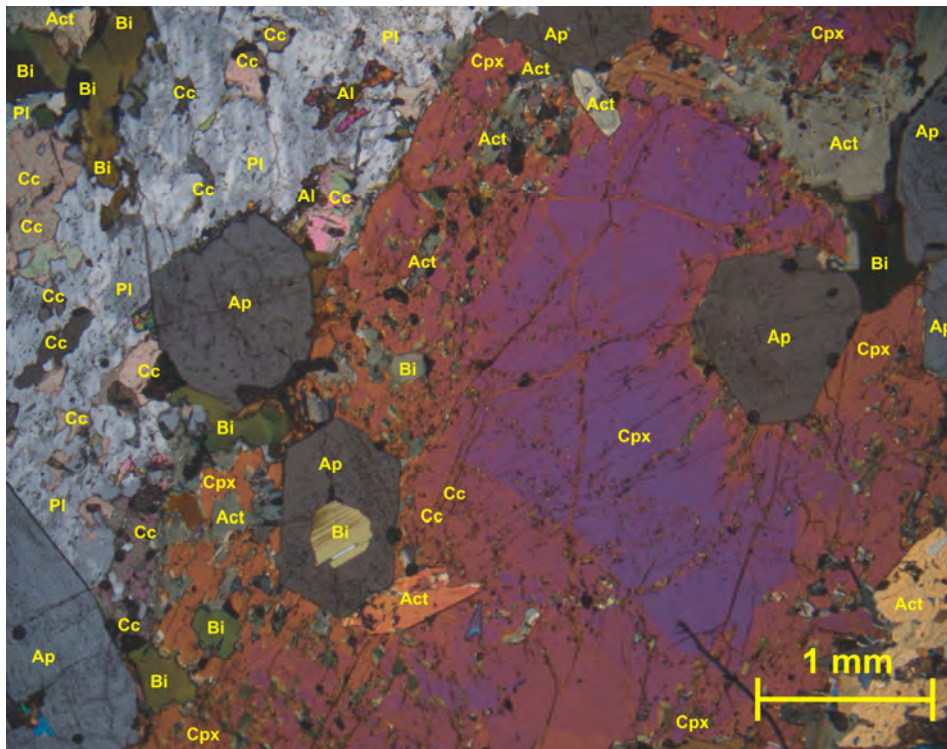


Figure 21. Apatite crystals (Ap) occurring intimately intergrown with biotite (Bi) and augite (Cpx), all of them showing incipient replacement by actinolite (Act) and aggregates of sodic plagioclase (Pl), calcite (Cc) and allanite (Al). Partly crossed polars. Bio-CPx of sample SKM 111.

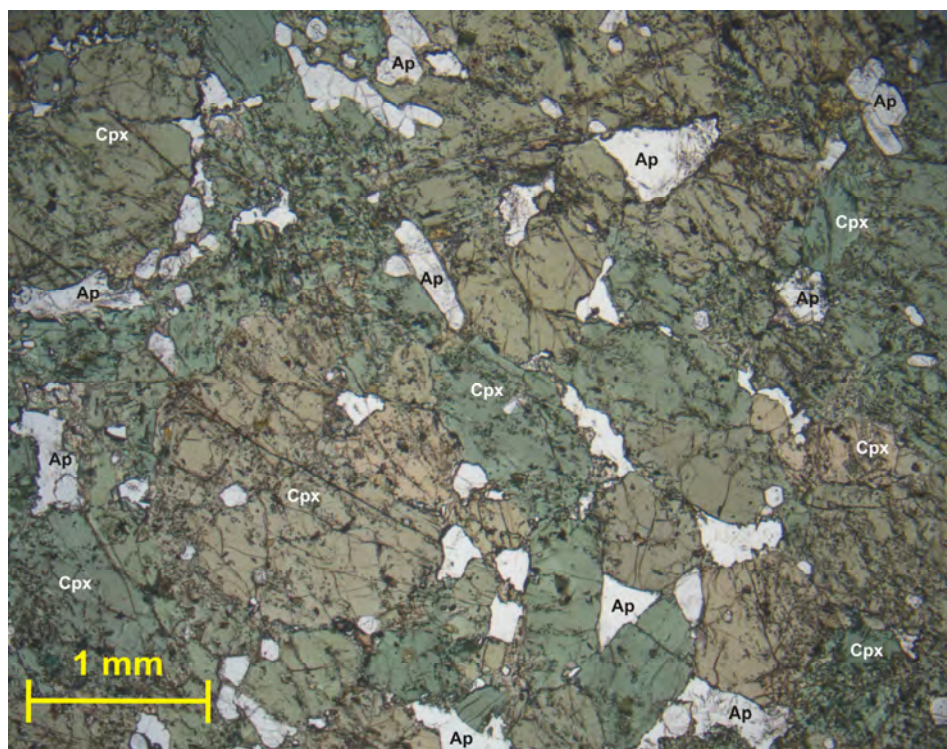


Figure 22. Interstitial grains and aggregates of apatite (Ap) in biotite-poor pyroxenite composed of light green augite (Cpx). The latter carries, as in Figure 21, inclusions of apatite. MPx of sample SKM 12.

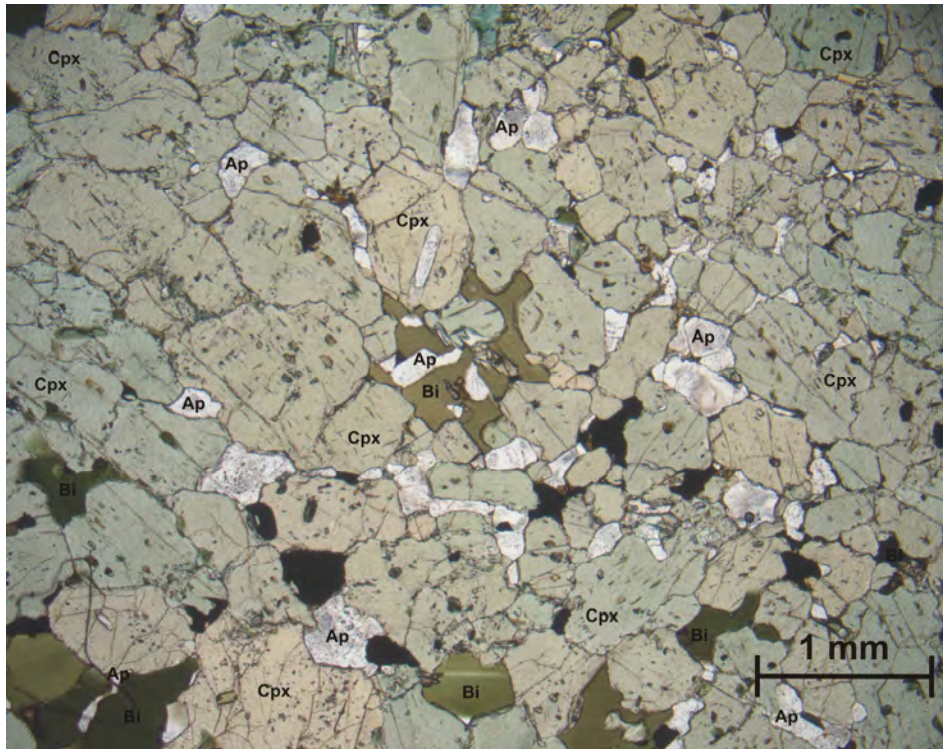


Figure 23. Medium-grained pyroxenite composed of augite (Cpx) with interstitial grains and aggregates of apatite (Ap), metasomatic green biotite (Bio) and opaques (black, pyrite and chalcopyrite). Some of the apatite occurs as inclusions both in augite and biotite. Bio-MPx of sample 47656 (Kårbøl junction).

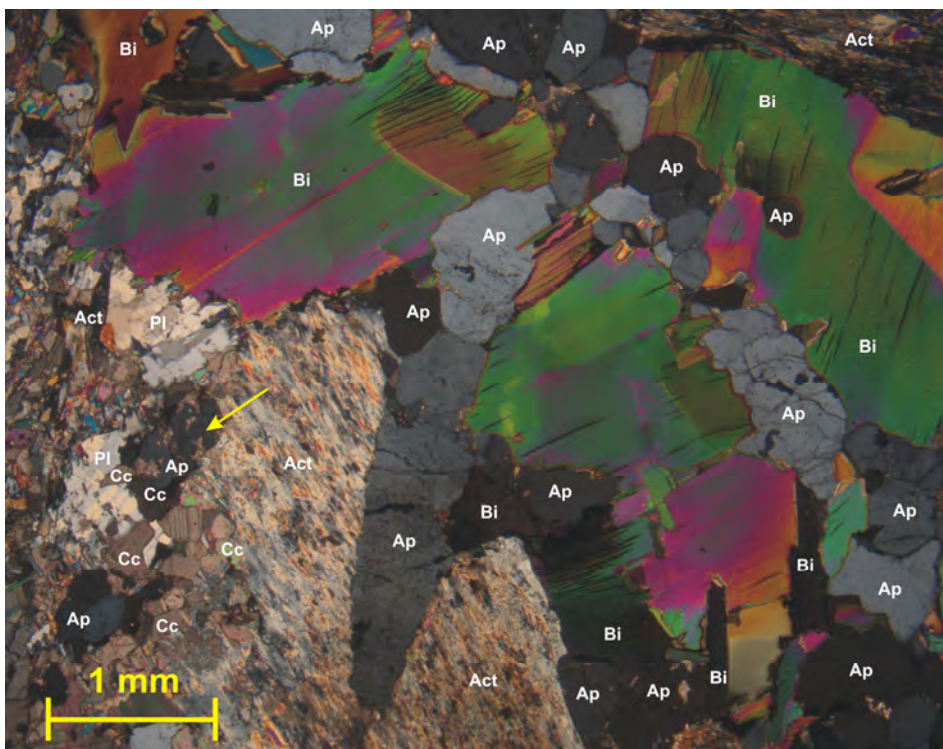


Figure 24. Elongated aggregates and disseminated single grains of apatite (Ap) in weakly deformed brownish green biotite (Bi) and a formerly augite crystal pseudomorphically replaced by fibrous aggregates of actinolite (Act). Left part of figure shows fine-grained aggregates of actinolite, calcite (Cc) and sodic plagioclase (Pl). Notice the apatite aggregates being replaced by calcite along grain boundaries (arrow) and biotite above by sodic plagioclase. Partly crossed polars. Bio-CPx of sample 47659 (Kårbøl junction).

3.2 The Hopsfjellet massif

The southern part of the massif is more or less continuously exposed along the main road (R80) over a distance of 1.5 km. It comprises a penetratively foliated and folded sequence of grey to greenish grey schistose ultramafites. They are composed of variable amounts of serpentine, talc, chlorite, amphibole (including anthophyllite) and locally garnet. They frequently show development of fine-scale banding possibly representing primary layering as indicated by the presence of fine-grained cherty bands in rusty zones with sparse dissemination of sulphides. The impression is that the ultramafic rocks are part of a layered mafic-ultramafic volcanic sequence as suggested by Gustavson (1994) who was the first to map and briefly describe the massif. Since the sampled ultramafic rocks have no features in common with those constituting the Misværdal massif, further work was regarded as unwarranted.

4. ANALYTICAL RESULTS

4.1 Misværdal

The major and trace element analyses show that the pyroxenites are generally enriched in P, Sr, Ba, Zr, Th, Nb and REE (max. 0.12 % REE), typical of alkaline ultramafic rocks. They are generally low in Ti (normally <1.2 TiO₂ %), as well as Cr and Ni. Since no visible grains of Fe-Ti oxides have been observed, it appears that Ti is mostly silicate-bound. The pyroxenites can be classified as potassic to ultra-potassic by their potassium contents of up to 8.2 % K₂O and with K₂O/Na₂O ratios mostly in the range 1-20 (average 7.2). They contain up to 0.14 % Y+REE. The light REE (La and Ce) that are dominant in this group of elements appear to increase with increasing P₂O₅. The weight % ratios of P₂O₅/ΣREE are in the range 22-74. This means that a concentrate composed totally of apatite would theoretically contain a maximum of 0.6-1.9 % REE. However, the possible contribution of REE from allanite (epidote mineral with abundant Ce+La) that occur in the samples (see Figure 19) suggests that the REE contents of apatite fall in the lower part of this range.

The sampled carbonate rocks are all low in Sr (<0.18 %), suggesting that they represent sedimentary carbonates or marbles. One carbonatite dyke sampled in 2006 yields 0.8 % Sr, typical for this group of magmatic rocks (Figure 12).

The analytical data listed in Appendix 1 together with calculated apatite contents as fluor-apatite (P₂O₅ % x 2.37) show that the pyroxenites are generally enriched in P₂O₅ and apatite. The total number of analyses of pyroxenites and gabbros (106) yields an arithmetic average of 2.1 % P₂O₅ or 5 % apatite for these rocks (Table 2). This table also shows that 16 samples out of 106 or 15 % of the samples contain more than 4 % P₂O₅ with an average of 5.5 % P₂O₅. 9 % of the analyses (10 samples), i.e. those with more than 5.0 % P₂O₅ give an average of 6.1 % P₂O₅ with a maximum of 6.6 % P₂O₅. In view of the ultimate goal of defining average grades exceeding 6 % P₂O₅ this is a very promising result that warrants follow-up work.

The distribution of P₂O₅ and calculated contents of apatite in the Misværdal massif are shown in Figures 25 and 26, respectively. These figures show that rocks containing more than 4.2 % P₂O₅ or 10 % apatite appear to be missing in the southern pyroxenite massif in contrast to the northern body where they are rather evenly distributed. This distribution is largely lithologically controlled since 80 % of the samples containing more than 4.2 % P₂O₅ (15 samples) are derived from coarse-grained mafic-ultramafic rocks with the exception of three that represent biotite-altered and/or feldspar veined/infiltrated MPx (Figure 27). This lithological control of the ore-grade enrichment of apatite is of crucial importance when planning further exploration steps.

Table 2. Statistical data for 107 analyses of P₂O₅ in mafic-ultramafic rocks of the Misværdal massif, excluding analyses of samples from globulites, syenites and wall rocks (gneisses, marbles, soapstones and granitoids). Data taken from Appendix 2.

P2O5 % RANGE	NUMBER OF SAMPLES	AVERAGE FOR VALUES > MIN.	FREQUENCY %	CUMULATIVE % >MIN. VALUE
6.6-6.0	6	6.43	5.6	5.6
5.0-5.9	4	6.14	3.7	9.3
4.0-4.9	6	5.49	5.6	14.9
3.0-3.9	10	4.73	9.4	24.3
2.0-2.9	15	3.87	14.0	38.3
1.0-2.9	35	2.74	32.7	71.0
0.0-0.9	31	2.10	29.0	100.0

When the analytical values are grouped according to lithologies and their sub-types as in Appendix 3 and Table 3, it becomes apparent that the individual lithological sub-types show a large spread in P₂O₅ values. An attempt to illustrate this is given in Figure 28. This shows that closely spaced samples from the same lithological unit such as the pairs SKM 2 and 110 (R812 north of Nonsåsen), SKM 25 and 26 (Middagsåsen), SKM 111 and 38673 (Brentliknubben) and SKM 90 and 95 (east of Skard) both give very high values and lower ones with average grades of 5.2, 4.1, 4.7 and 4.8 % P₂O₅, respectively.

Since higher average grades are needed if any exploitation is considered, this is the first obstacle to be solved by dense sampling in profiles across well-exposed parts of the coarse-grained units. This is necessary in order to evaluate how apatite is distributed in the individual units, erratically or evenly.

An unaltered and chilled dyke of medium-grained pyroxenite (SKM 112) yielded 2.5 % P₂O₅ that are considered to roughly represent the concentration in the original potassic MPx magma. With such high concentrations in the parent magma any residual melt derived from it would be expected to be very rich in P₂O₅. In addition, when considering the size of the northern body of the Misværdal massif (~6 km²) in relation to present results, there is still a possibility for reaching the ultimate goal of the project.

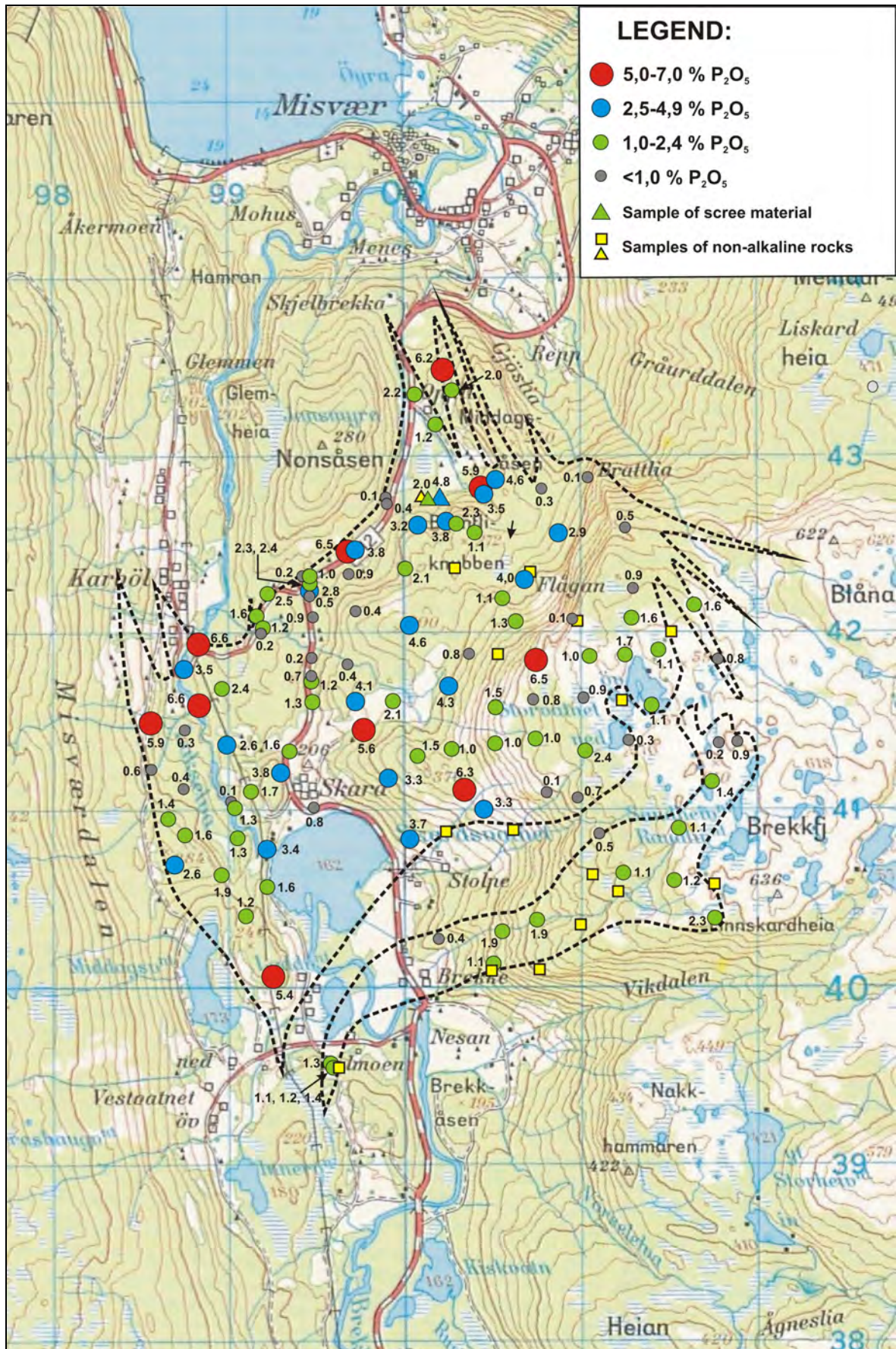


Figure 25. Map showing the distribution of P_2O_5 in the Misværdalen pyroxenite massif. All samples of alkaline rocks collected during the period 2006-2008 are shown.

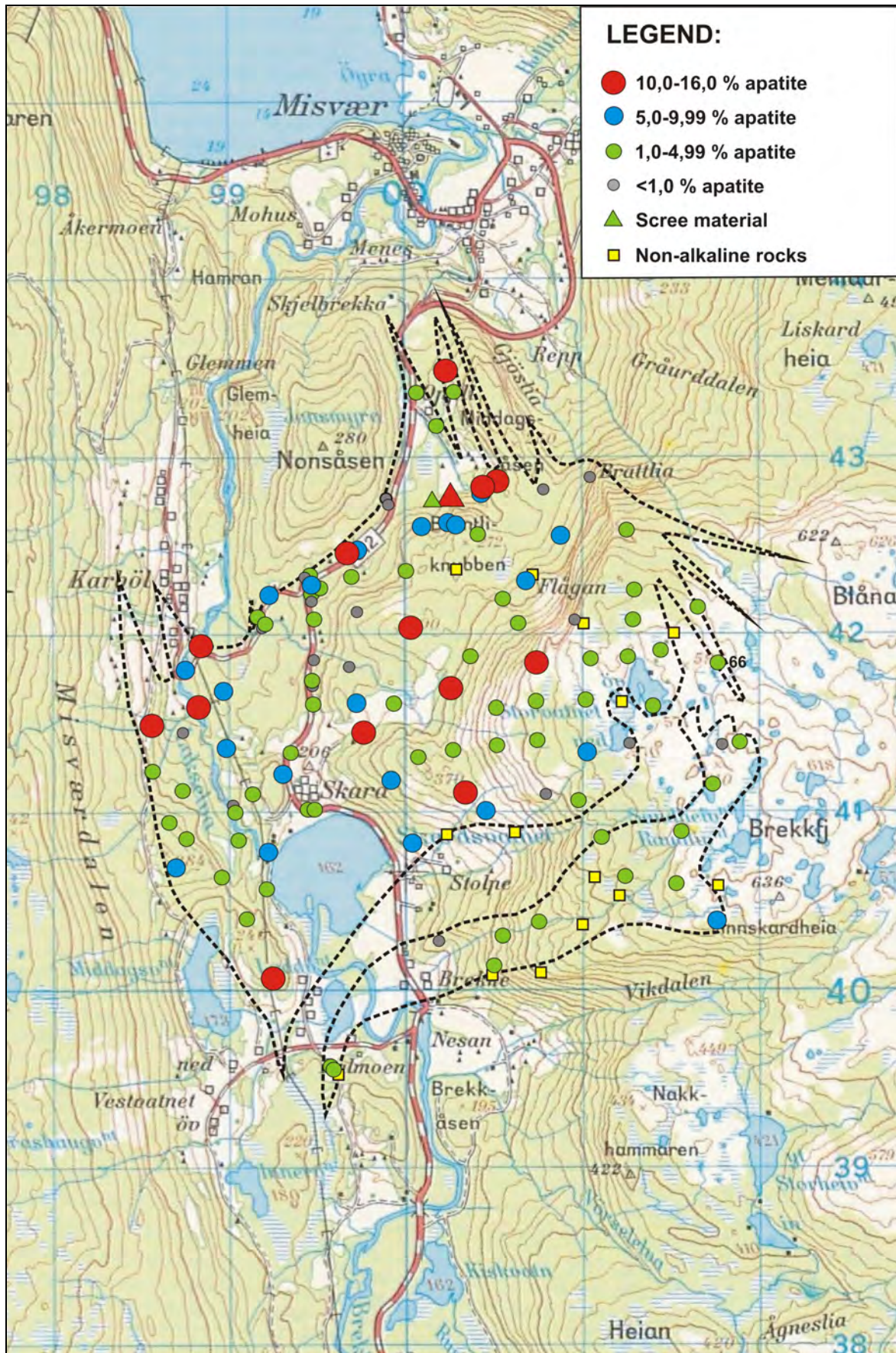


Figure 26. Map showing the distribution of calculated apatite contents in the Misværdal pyroxenite massif. All samples of alkaline rocks collected during the period 2006-2008 are shown.

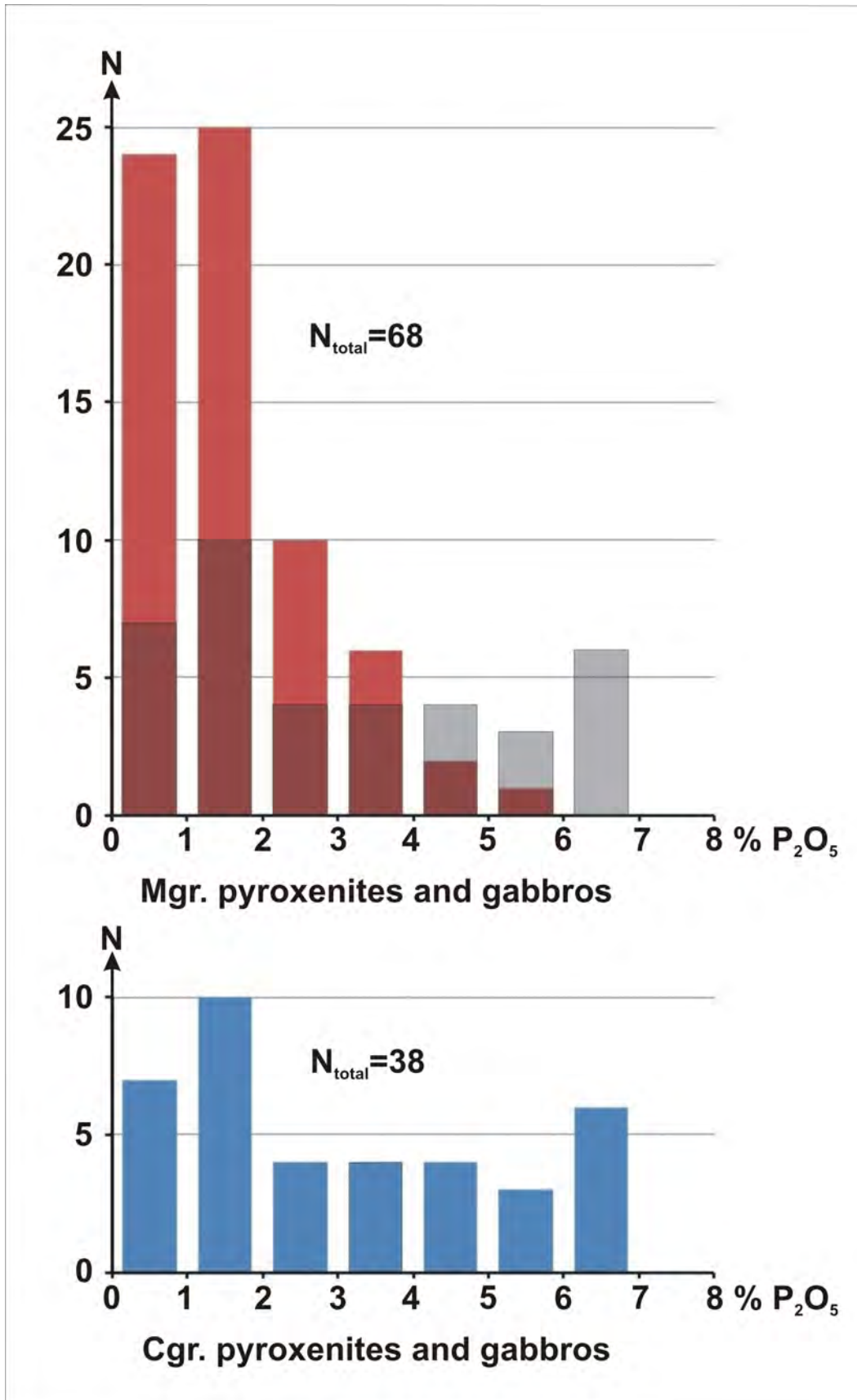


Figure 27. Histograms showing number (*N*) of samples within given 1 % intervals of weight % P₂O₅. Medium-grained rocks in red (top) compared to coarse-grained rocks in grey (top) that are shown separately in dark blue (bottom).

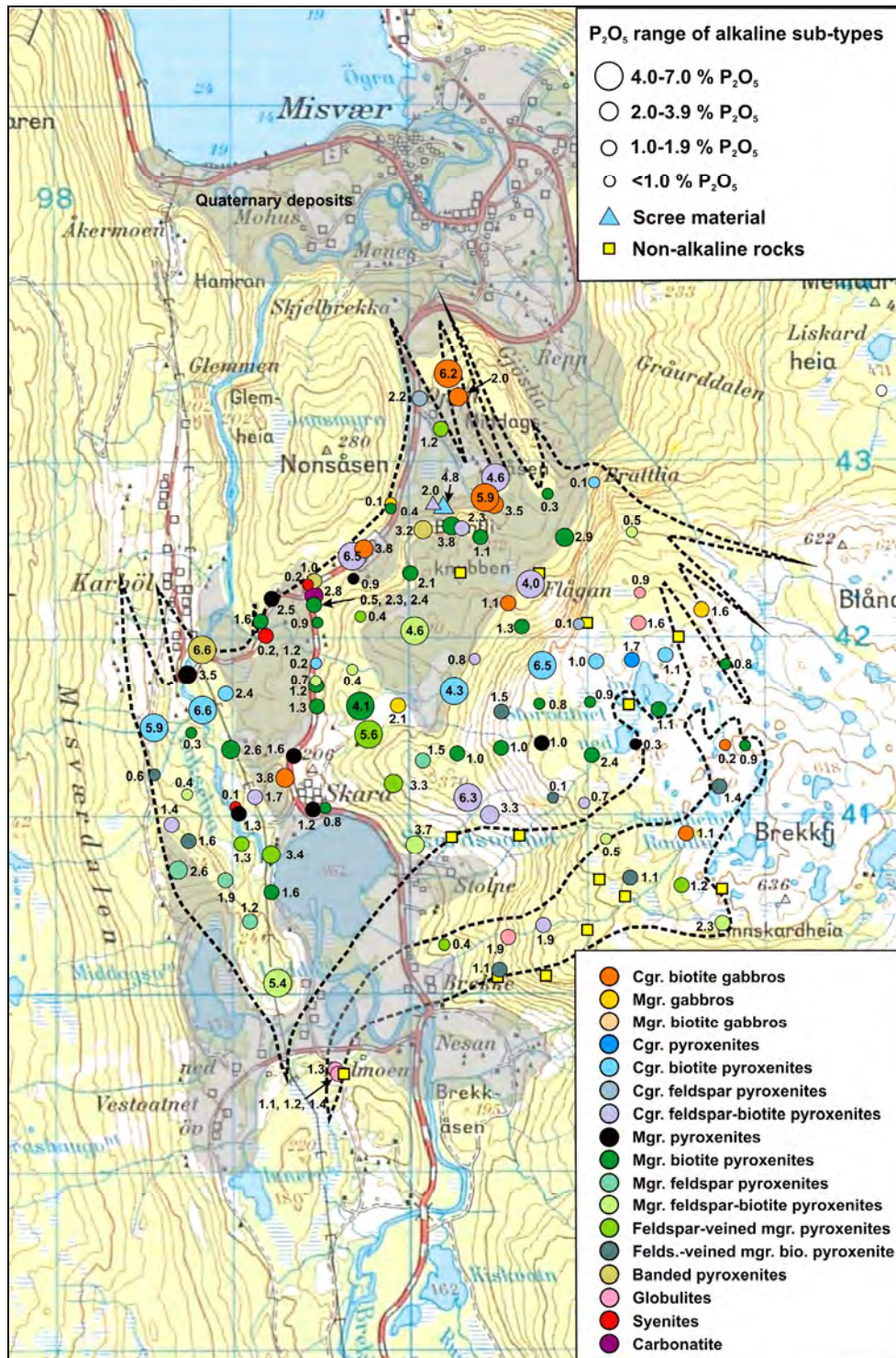


Figure 28. Map showing the distribution of P₂O₅ in the Misværdalen pyroxenite massif in relation to type of alkaline rock in the analysed sample. All samples of alkaline rocks collected during the period 2006-2008 are shown.

4.2 Hopsfjellet

The samples returned analytical values of less than 0.13 % P₂O₅ confirming the impression that the massif comprises rocks with no apparent apatite potential.

Table 3. Statistical data of P_2O_5 contents of analysed rocks sampled in the period 2006-2008. *N*: number of analysed samples, *1STDV*: one standard deviation. Summary of data presented in Appendix 3 where the P_2O_5 values are sorted according to lithology or lithology or lithological code given in the sample description in Appendix 1 and in the text.

ROCK TYPE	N	ARITMETRIC AVERAGE	1 STDEV	RANGE	
				MIN.	MAX.
Misværdal:					
All types of coarse-grained pyroxenites	30	3.01	2.22	0.10	6.55
All types of coarse-grained gabbros	8	3.01	2.26	0.22	6.16
All types of medium-grained pyroxenites	62	1.61	1.19	0.09	5.58
All types of medium-grained gabbros	6	1.37	0.73	0.12	2.06
Subtypes of alkaline rocks:					
Coarse-grained (cgr.) pyroxenite	1				1.71
Cgr. biotite pyroxenite	12	3.49	2.43	0.11	6.55
Cgr. feldspar pyroxenite	2	1.14	1.46	0.10	2.17
Cgr. feldspar-biotite pyroxenite	13	2.78	2.01	0.68	6.47
Cgr. banded biotite pyroxenites	1				1.73
Cgr. banded feldspar-biotite pyroxenite	1				6.63
Coarse-grained (cgr.) gabbro	1				1.08
Cgr. biotite gabbro	7	3.28	2.29	0.22	6.16
Medium-grained (mgr.) pyroxenite	8	1.68	0.99	0.26	3.48
Mgr. biotite pyroxenite	25	1.48	1.04	0.29	4.11
Mgr. feldspar pyroxenite	4	1.83	0.61	1.23	2.64
Mgr. feldspar-biotite pyroxenite	7	1.76	1.78	0.35	4.56
Mgr. carbonate-biotite pyroxenite	1				1.15
Mgr. feldspar-veined pyroxenite	8	2.09	1.82	0.35	5.58
Mgr. feldspar-veined biotite pyroxenite	7	1.07	0.55	0.09	1.64
Mgr. banded biotite pyroxenite	1				0.94
Mgr. banded feldspar-biotite pyroxenite	1				3.20
Medium-grained (mgr.) gabbro	3	1.27	1.02	0.12	2.06
Mgr. biotite gabbro	2	1.39	0.72	0.88	1.90
Mgr. banded biotite gabbro	1				1.64
Carbonatite	1				2.75
Syenite	4	0.36	0.48	0.07	1.21
Globulite	5	1.23	0.11	1.08	1.37
Wallrocks:					
Granitoids	4	0.53	0.30	0.26	0.89
Marbles	10	0.20	0.22	0.02	0.70
Gneisses	2	0.15	0.06	0.10	0.19
Soapstones	2	0.03	0.01	0.02	0.03
Hopsfjellet:					
Serpentine-talc-chlorite schists	5	0.10	0.02	0.08	0.13

5. ASSESSMENT OF THE APATITE POTENTIAL

The P_2O_5 analyses strongly indicate that high apatite grades are expected to occur in the coarse-grained pyroxenites and gabbros that in a number of cases occur together in the coarse-grained units. The tonnage potential is therefore dependent on the thickness and strike extent of these units, which are most widespread in the northern pyroxenite body where the potential is considered to be best.

The low degree of exposures in many parts of the northern body makes it impossible to decide if the coarse-grained units form continuous layers, trains of smaller lenses, dykes that bifurcate or more irregularly shaped bodies. This makes it difficult to join the different sampled outcrops into properly defined units. However, based on limited field observations, an attempt has been made to define potential apatite-rich zones as shown in Figure 29 where they appear to form N- to NW-trending plate-shaped bodies in the MPx.

Figure 29 depicts 4 potential units containing rocks returning high- to medium-levels of P_2O_5 . Each of them has an estimated thickness in the range 50-200 m and a strike extent of 1-2 km, i.e. 180 000-25000 m² for each or a total outcrop area of about 900 000 m². Although the defined zones may appear to be speculative, they suggest that the ultimate goal of the project is within reach. Samples collected from these zones yield averages in the range 3-5 % P_2O_5 . When assessing these grades, it has to be remembered that the analysed samples represent a very small area, and that nothing is known about the internal distribution of apatite on dm, meter and decameter scales in the units. Thus it is nearly impossible to make a true assessment of average grades at the present state of knowledge.

Other high-grade samples outside the potential units represent narrow CPx zones (1-20 m) represented by the two samples 0.5-1 km west of the lake, Øvre Storvatn and those along the river, Lakselv and west of it. The MPx samples returning high P_2O_5 values such as the sampling points NNE of Skard were collected in very small outcrops and their significance is therefore difficult to assess. None of them appears to be part of the potential zones.

Highly potassic mafic-ultramafic volcanites have long been known to be enriched in P_2O_5 (>1%; Carmichael et al. 1974). Biotite-rich mafic-ultramafic complexes with associated subordinate carbonatite intrusions (melilitite-type) are the main host for apatite ores such as those in the Kovdor and Phalaborwa complexes (Mitchell 2005). In both of these complexes the apatite ore bodies are represented by intrusions of phoskorite or apatite-magnetite-olivine rocks. In Phalaborwa or Palaborwa the phoskorites intrude phlogopite- (biotite-) and apatite-rich pyroxenites and ultramafic pegmatoids (Guilbert and Park 1986) comparable to those in the Misværdal massif where phoskorites appear to be missing.

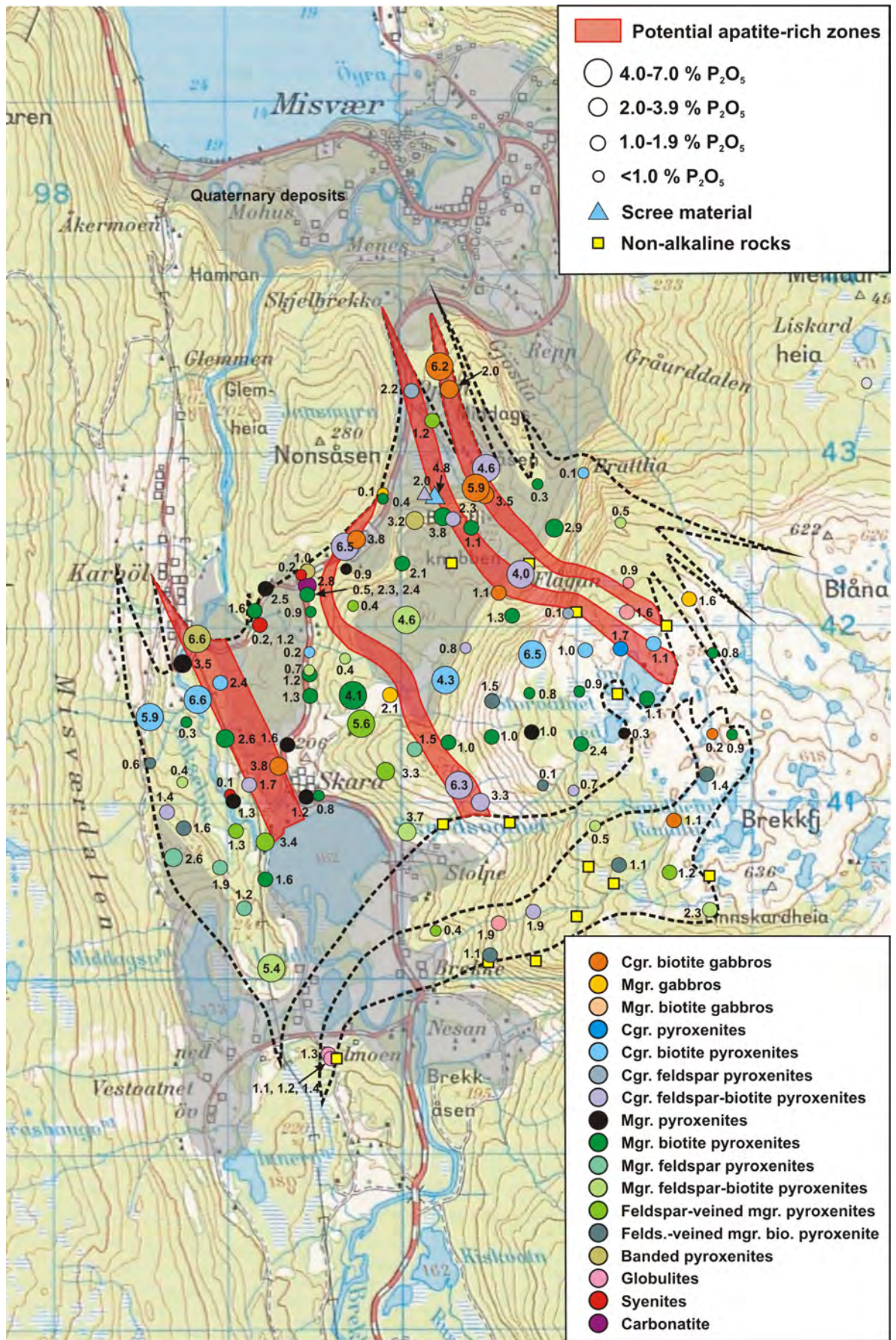


Figure 29. Map showing the location of potential apatite-rich zones (red) in the Misværdal massif that deserve follow-up work.

6. AEROMAGNETIC SIGNATURES

The Misværdal pyroxenite massif is recognised by a weak, but distinct subsircular magnetic anomaly on maps compiled from high-altitude aeromagnetic data in the NGU database (Figure 30). The anomaly confirms the westerly dip of the northern pyroxenite, whereas the southern MPx-dominated body show weak magnetic response. The anomaly peak is, however, located outside and west of the northern pyroxenite body in an area carrying low-magnetic gneisses and marbles at surface west of the river Lakselva. The pyroxenites at the surface are generally devoid of visible Fe-oxides and carry only trace amounts of very fine-grained magnetite and associated Fe-sulphides precipitated during the metasomatic stage when carbonatite dykes, some rich in magnetite, were emplaced. This may suggest either that the northern body may become increasingly magnetic towards depth due to the presence of phosphorites or that some of the marbles at the surface may represent deformed magnetite-bearing carbonatites.

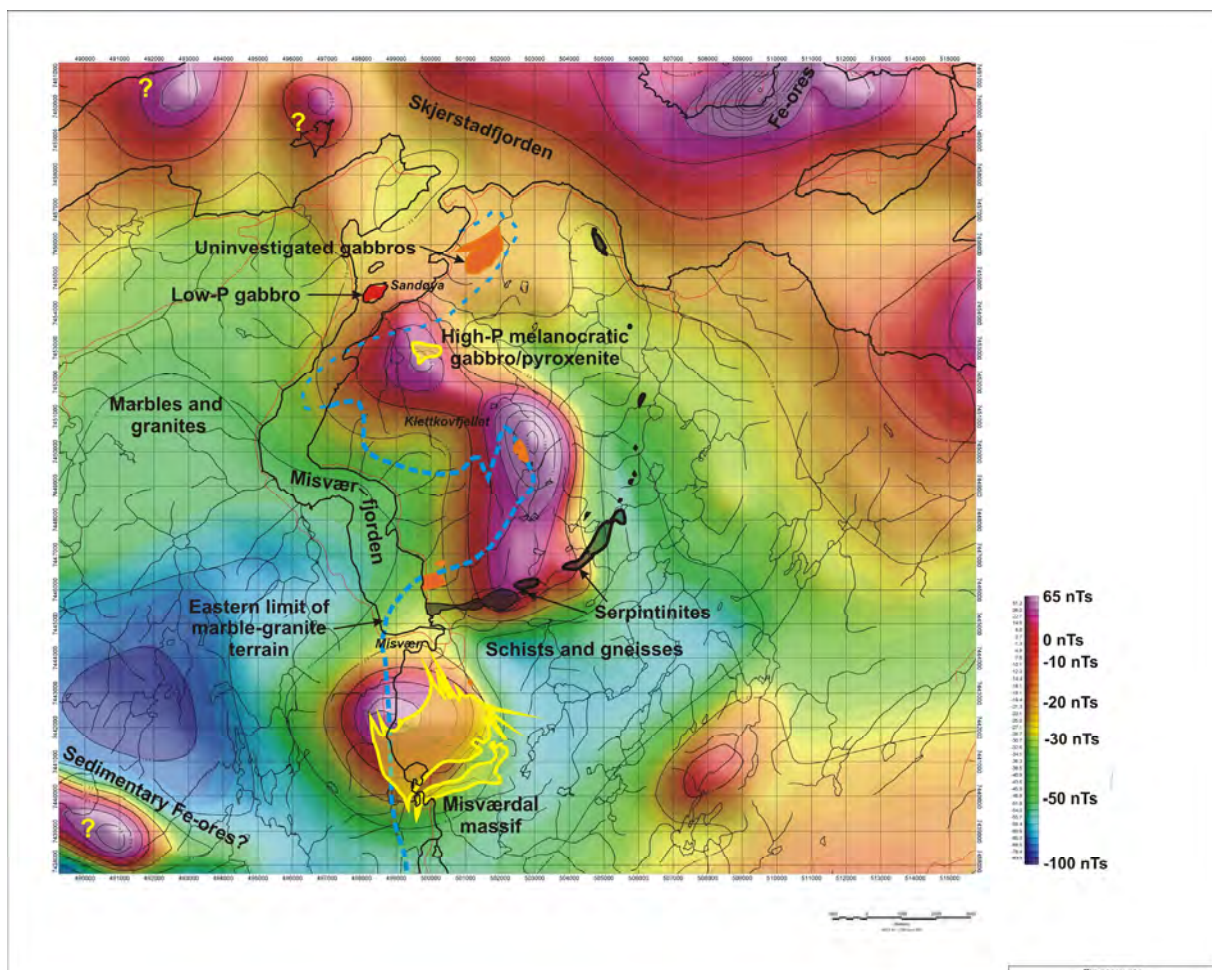


Figure 30. Aeromagnetic anomaly map showing the location of mafic-ultramafic bodies in the Misvær area. Map compiled from magnetic data in the NGU geophysical database and bedrock map Misvær, 1:50000 (Solli et al. 1992).

The Misværdal anomaly represents the southernmost of a train of comparable anomalies that can be followed northwards on the eastern side of Misværfjord towards Skjerstadvjord and onwards to its northern shore. In this area there are also several mafic-ultramafic bodies as shown in Figure 24. Some of these coincide with the anomalies, whereas others are situated outside them. Samples collected by Nordland Mineral from the weakly magnetic serpentinite bodies east of Misvær and the gabbro at Sandøya in the north contain less than 0.3 % P_2O_5 . In contrast, the body of melanocratic gabbro/pyroxenite inside the magnetic anomaly on the northwestern side of Klettkovfjellet yields analyses in the range 1.2-1.4 % P_2O_5 . Thus it appears that intrusions with anomalous contents of phosphorus are distinctly magnetic and therefore the magnetic anomalies may represent guides to apatite ore. In general, detailed bedrock geology is missing for the areas covered by the magnetic anomalies and the exact size and nature of the marked intrusions are therefore unknown. Since the magnetic anomaly areas may carry phosphorus-rich pyroxenite and carbonatite intrusions, they have the potential of hosting additional reserves to the Misværdal massif. Thus it is recommended that they are followed up by ground geological surveys.

7. CONCLUSIONS

The following conclusions can be drawn from the data collected so far:

- The Hopsfjellet ultramafic massif comprises a sequence of meta-volcanic rocks low in phosphorus and appears to have no apatite ore potential.
- The Misværdal massif comprises two intrusive bodies of medium-grained pyroxenites containing units of coarse-grained pyroxenites, as well as dykes of alkali-feldspar syenites and minor lense-shaped intrusions of carbonatite. The rocks have been overprinted by strong alkali metasomatism, possible fenitisation, generating pyroxenites rich in biotite and/or alkali feldspar.
- The pyroxenites and gabbros are strongly enriched in phosphorus, with an average content of 2.1 % P_2O_5 or 5 weight % apatite (107 samples).
- Nearly 15 % of the collected samples of mafic-ultramafic rocks contain more than 4 % P_2O_5 with an average of 5.5 % P_2O_5 . 9 % of the analyses, i.e. those with more than 5.0 % P_2O_5 or 10 samples, give an average of 6.1 % P_2O_5 with a maximum of 6.6 % P_2O_5 .
- The P_2O_5 -rich samples (>10 % apatite) are nearly invariably derived from coarse-grained pyroxenite units, emphasizing the lithological control of the apatite enrichment.
- 4 potentially apatite-rich coarse-grained units can speculatively be defined, each comprising thicknesses in the range 50-200 m and strike extensions of 1-2 km, i.e. 180 000-250000 m^2 for each unit, roughly coinciding with the lower limit of 200 000 m^2 for a potential target area.
- The P_2O_5 contents of samples collected in the coarse-grained units are highly variable. Thus the estimation of average grades of P_2O_5 in these units is difficult. Neighbouring samples in the same unit yield averages in the range 4.1-5.2 % P_2O_5 , below the ultimate goal of 6 % P_2O_5 or more.

8. RECOMMENDATIONS

Several recommendations can be given regarding further follow-up work, both on a local and regional scale. Below they are listed in order of priority.

1. Microprobe and laser ablation ICP-MS analyses of chlorine and other unwanted contaminants should be conducted.
2. An attempt should be made to map the individual coarse-grained units inside the Misværdal massif in more detail in order to get a better understanding of their shape and dimensions.
3. Those units that exceed thicknesses of 50 m should be sampled systematically in selected traverses that are well exposed. This is done to get better estimates of their average grades and to determine the variations in P₂O₅ contents on dm and m scales. Dense sampling by the use of a portable core sampler (35 cm x 38 mm cores) is recommended.
4. The samples should also be used for magnetic susceptibility measurements in order to determine potentially contrasting magnetic signatures from the different rock types, especially the coarse-grained pyroxenites, to be utilised in magnetic ground surveys in areas with thick overburden.
5. These steps can be conducted without having to involve of a high number of landowners that have the mineral rights to about 67 different properties that cover the ground in the Misværdal massif.
6. The magnetic anomalies to the north and east of the Misvær fjord should be surveyed for potential apatite-bearing rocks that should be sampled for analysis.

9. REFERENCES

- Carmichael, I.S.E., Turner, F.J. and Verhoogen, J. 1974: *Igneous petrology*. McGraw-Hill International Series in the earth and planetary sciences, McGraw-Hill Book Company, New York, 739 pp.
- Farrow, C.M. 1994: *The geology of the Skjerstad area, Nordland, North Norway*. University of Bristol, PhD thesis, 186 pp.
- Gjelle, S. 1988: *Geologisk kart over Norge. Berggrunnskart SALTDAL, 1:250 000*. Norges geologiske undersøkelse.
- Guilbert, J.M. and Park, C.F., Jr. 1986: *The geology of ore deposits*. W.H. Freeman and Co., New York, NY, United States, 985 pp.
- Gustavson, M. 1994: *Bodø 2029 IV. Berggrunnskart, M 1:50 000, med beskrivelse*. Norges geol. unders. skr. 144, 20 pp.
- Gustavson, M. 1996: *Geologisk kart over Norge. Berggrunnskart SULITJELMA, M 1:250 000*. Norges geologiske undersøkelse.
- Gustavson, M. and Blystad, P. 1995: *Geologisk kart over Norge. Berggrunnskart*

- BODØ, 1:250 000. Norges geologiske undersøkelse.
- Gustavson, M. and Gjelle, S. 1992: Geologisk kart over Norge. Berggrunnskart
MO I RANA, 1:250 000. Norges geologiske undersøkelse.
- Mitchell, R. H. 2005: Carbonatites and carbonatites and carbonatites. The Canadian
Mineralogist 43, 2049-2068.
- Solli, A., Farrow, C.M. and Gjelle, S. 1992: MISVÆR 2029 II. Berggrunnskart,
M 1:50 000. Norges geologiske undersøkelse.

Appendix 1. Sample weight in kilogram and analytical values for P_2O_5 in weight % listed in numerical order of samples for the period 2006-2008. 4A = ICP-ES analyses and 4B = ICP-MS analyses. Litho. codes are given in Appendix 5 together with transformation factors for the calculation of weight % apatite.

SAMPLE	SAMPLE WEIGHT KG.	4A P_2O_5 %	4B P_2O_5 %	4A+B P_2O_5 %	CALC. % APATITE	LITHO. CODE
PRØVER 2008: MISVÆRDAL						
SKM-01	1.73	1.73	N.A.	1.73	4.1	Bnd-Bio-CPx
SKM-02	1.84	N.A.	6.47	6.47	15.3	FspBio-CPx
SKM-03	1.95	N.A.	0.12	0.12	0.3	MGb
SKM-04	2.08	2.17	N.A.	2.17	5.1	Fsp-CPx
SKM-05	2.44	1.58	N.A.	1.58	3.7	Bio-MPx
SKM-06	2.14	6.63	N.A.	6.63	15.7	Bnd-FspBio-CPx
SKM-07	2.13	N.A.	2.41	2.41	5.7	Bio-CPx
SKM-08	2.42	2.59	N.A.	2.59	6.1	Bio-MPx
SKM-09	1.23	N.A.	1.32	1.32	3.1	MPx
SKM-10	2.56	1.74	N.A.	1.74	4.1	FspBio-CPx
SKM-11	1.58	1.61	N.A.	1.61	3.8	Bio-MPx
SKM-12	1.76	1.33	N.A.	1.33	3.2	Vnd-Fsp-MPx
SKM-13	1.43	1.64	N.A.	1.64	3.9	Vnd-FspBio-MPx
SKM-14	1.37	2.64	N.A.	2.64	6.3	Fsp-MPx
SKM-15	1.21	1.92	N.A.	1.92	4.6	Fsp-MPx
SKM-16	1.47	1.23	N.A.	1.23	2.9	Fsp-MPx
SKM-17	1.85	5.42	N.A.	5.42	12.8	Bio-CPx
SKM-18	1.54	N.A.	0.49	0.49	1.2	FspBio-MPx
SKM-19	1.37	0.88	N.A.	0.88	2.1	Bio-MGb
SKM-20	1.47	0.10	N.A.	0.10	0.2	Fsp-CPx
SKM-21	1.62	0.02	N.A.	0.02	0.0	Marble
SKM-22	1.97	1.64	N.A.	1.64	3.9	Bnd-Bio-MGb
SKM-23	0.93	0.17	N.A.	0.17	0.4	Marble
SKM-24	2.24	1.63	N.A.	1.63	3.9	MGb
SKM-25	2.37	6.16	N.A.	6.16	14.6	Bio-CGb
SKM-26	1.61	N.A.	2.03	2.03	4.8	Bio-CGb
SKM-27	1.42	0.29	N.A.	0.29	0.7	Bio-MPx
SKM-28	1.85	0.11	N.A.	0.11	0.3	Bio-CPx
SKM-29	1.98	4.58	N.A.	4.58	10.9	FspBio-CPx
SKM-30	1.69	3.28	N.A.	3.28	7.8	Vnd-Fsp-MPx
SKM-31	1.75	0.93	N.A.	0.93	2.2	Bio-MPx
SKM-32	2.00	N.A.	0.75	0.75	1.8	Bio-MPx
SKM-33	1.58	6.46	N.A.	6.46	15.3	Bio-CPx
SKM-34	1.86	1.02	N.A.	1.02	2.4	Bio-CPx
SKM-35	1.90	1.71	N.A.	1.71	4.1	CPx
SKM-36	2.31	0.02	N.A.	0.02	0.0	Soapstone
SKM-37	1.98	0.98	N.A.	0.98	2.3	MPx
SKM-38	2.59	0.94	N.A.	0.94	2.2	Bnd-Bio-MPx

SAMPLE	SAMPLE WEIGHT KG.	4A P₂O₅ %	4B P₂O₅ %	4A+B P₂O₅ %	CALC. % APATITE	LITHO. CODE
SKM-39	1.86	2.06	N.A.	2.06	4.9	MPx
SKM-40	1.79	3.20	N.A.	3.20	7.6	Bnd-FspBio-Px
SKM-41	1.75	3.77	N.A.	3.77	8.9	Bio-MPx
SKM-42	1.15	2.33	N.A.	2.33	5.5	FspBio-CPx
SKM-43	1.07	0.02	N.A.	0.02	0.0	Marble
SKM-44	2.06	N.A.	0.89	0.89	2.1	Bio-MPx
SKM-45	1.62	N.A.	0.24	0.24	0.6	Bio-CPx
SKM-46	2.24	N.A.	1.27	1.27	3.0	Bio-MPx
SKM-47	1.72	1.64	N.A.	1.64	3.9	MPx
SKM-48	2.53	3.75	N.A.	3.75	8.9	Bio-CGb
SKM-49	2.08	0.75	N.A.	0.75	1.8	Bio-MPx
SKM-50	1.95	3.36	N.A.	3.36	8.0	Vnd-Fsp-MPx
SKM-51	1.73	5.58	N.A.	5.58	13.2	Vnd-Fsp-MPx
SKM-52	2.01	4.11	N.A.	4.11	9.7	Bio-MPx
SKM-53	2.17	0.35	N.A.	0.35	0.8	FspBio-MPx
SKM-54	2.47	0.38	N.A.	0.38	0.9	Vnd-Fsp-MPx
SKM-55	2.37	3.48	N.A.	3.48	8.2	MPx
SKM-56	1.92	6.55	N.A.	6.55	15.5	Bio-CPx
SKM-57	2.14	0.43	N.A.	0.43	1.0	FspBio-MPx
SKM-58	1.98	N.A.	1.41	1.41	3.3	FspBio-CPx
SKM-59	2.12	0.64	N.A.	0.64	1.5	Vnd-FspBio-MPx
SKM-60	2.47	5.93	N.A.	5.93	14.1	Bio-CPx
SKM-61	1.99	0.32	N.A.	0.32	0.8	Bio-MPx
SKM-62	1.78	0.32	N.A.	0.32	0.8	Granitoid
SKM-63	1.65	0.66	N.A.	0.66	1.6	PxGranitoid
SKM-64	1.89	0.18	N.A.	0.18	0.4	Marble
SKM-65	1.63	N.A.	1.11	1.11	2.6	Bio-CPx
SKM-66	2.03	0.80	N.A.	0.80	1.9	Bio-MPx
SKM-67	2.24	1.11	N.A.	1.11	2.6	Bio-MPx
SKM-68	2.03	N.A.	0.26	0.26	0.6	MPx
SKM-69	1.91	2.38	N.A.	2.38	5.6	Bio-MPx
SKM-70	1.79	N.A.	0.22	0.22	0.5	Bio-CGb
SKM-71	1.70	0.89	N.A.	0.89	2.1	Bio-MPx
SKM-72	1.58	N.A.	0.07	0.07	0.2	Syenite
SKM-73	1.56	1.42	N.A.	1.42	3.4	Vnd-FspBio-MPx
SKM-74	1.59	1.08	N.A.	1.08	2.6	CGb
SKM-75	1.93	0.46	N.A.	0.46	1.1	FspBio-MPx
SKM-76	1.74	1.12	N.A.	1.12	2.7	Vnd-FspBio-MPx
SKM-77	1.81	2.30	N.A.	2.30	5.5	FspBio-MPx
SKM-78	1.95	0.19	N.A.	0.19	0.5	Gneiss
SKM-79	2.03	1.17	N.A.	1.17	2.8	Vnd-Fsp-MPx
SKM-80	1.49	0.68	N.A.	0.68	1.6	FspBio-CPx
SKM-81	1.71	1.89	N.A.	1.89	4.5	FspBio-CPx

SAMPLE	SAMPLE WEIGHT KG.	4A P ₂ O ₅ %	4B P ₂ O ₅ %	4A+B P ₂ O ₅ %	CALC. % APATITE	LITHO. CODE
SKM-82	1.70	0.89	N.A.	0.89	2.1	PxGranitoid
SKM-83	1.76	1.90	N.A.	1.90	4.5	Bio-MGb
SKM-84	2.07	1.09	N.A.	1.09	2.6	Vnd-FspBio-MPx
SKM-85	1.77	0.21	N.A.	0.21	0.5	Marble
SKM-86	1.95	0.39	N.A.	0.39	0.9	Vnd-Fsp-MPx
SKM-87	1.87	0.09	N.A.	0.09	0.2	Vnd-FspBio-MPx
SKM-88	2.26	1.04	N.A.	1.04	2.5	Bio-MPx
SKM-89	2.34	1.51	N.A.	1.51	3.6	Vnd-FspBio-MPx
SKM-90	1.76	3.31	N.A.	3.31	7.8	FspBio-CPx
SKM-91	1.59	0.97	N.A.	0.97	2.3	Bio-MPx
SKM-92	1.97	4.32	N.A.	4.32	10.2	Bio-CPx
SKM-93	1.47	N.A.	2.06	2.06	4.9	MGb
SKM-94	2.12	1.51	N.A.	1.51	3.6	Fsp-MPx
SKM-95	1.62	6.32	N.A.	6.32	15.0	FspBio-CPx
SKM-96	1.93	1.09	N.A.	1.09	2.6	Bio-MPx
SKM-97	1.86	N.A.	2.94	2.94	7.0	Bio-MPx
SKM-98	2.03	1.08	N.A.	1.08	2.6	Bio-CGb
SKM-99	1.77	1.29	N.A.	1.29	3.1	Bio-MPx
SKM-100	1.83	0.80	N.A.	0.80	1.9	FspBio-CPx
SKM-101	2.34	4.56	N.A.	4.56	10.8	FspBio-MPx
SKM-102	1.45	0.04	N.A.	0.04	0.1	Marble
SKM-103	1.62	0.26	N.A.	0.26	0.6	Granitoid
SKM-104	1.88	3.74	N.A.	3.74	8.9	FspBio-MPx
SKM-105	2.27	0.17	N.A.	0.17	0.4	Marble
SKM-106	1.86	N.A.	4.01	4.01	9.5	FspBio-CPx
SKM-107	1.67	0.10	N.A.	0.10	0.2	Gneiss
SKM-108	1.48	1.22	N.A.	1.22	2.9	Vnd-Fsp-MPx
SKM-109	2.04	1.27	N.A.	1.27	3.0	Globulite
SKM-110	2.48	3.83	N.A.	3.83	9.1	Bio-CGb
SKM-111	2.40	N.A.	5.92	5.92	14.0	Bio-CGb
SKM-112	1.27	N.A.	2.47	2.47	5.9	MPx
PRØVER 2008: HOPSFJELLET						
HF-01	1.81	0.13	N.A.	0.13	0.3	Mg-rich schist
HF-02	1.20	0.09	N.A.	0.09	0.2	Mg-rich schist
HF-03	1.12	0.12	N.A.	0.12	0.3	Mg-rich schist
HF-04	1.49	0.09	N.A.	0.09	0.2	Mg-rich schist
HF-05	1.83	0.08	N.A.	0.08	0.2	Mg-rich schist
PRØVER 2007: MISVÆRDAL						
38667	N.D.	Brentliknubben1		4.78	11.3	Bio-CPx
38668	N.D.	Brentliknub.2		0.02	0.1	Marble
38669	N.D.	Brentliknub.3		0.70	1.7	Marble
38670	N.D.	Brentliknubben4		1.98	4.7	FspBio-CPx
38671	N.D.	Brentliknub.5		0.43	1.0	Marble

SAMPLE	SAMPLE WEIGHT KG.	4A P ₂ O ₅ %	4B P ₂ O ₅ %	4A+B P ₂ O ₅ %	CALC. % APATITE	LITHO. CODE
38672	N.D.	Brentliknub.6		0.03	0.1	Soapstone
38673	N.D.	Brentliknubben7		3.53	8.4	Bio-CPx
38674	N.D.	Nonshaugen		0.41	1.0	Bio-MPx
38675	N.D.	Skardbakken1		0.68	1.6	FspBio-CPx
38676	N.D.	Skardbakken2		1.15	2.7	CarbBio-MPx
PRØVER 2006: MISVÆRDAL						
47656	N.D.	Karbøl junction		2.37	5.6	Bio-MPx
47657	N.D.	Karbøl junction		0.53	1.3	Bio-MPx
47658	N.D.	Karbøl junction		0.20	0.5	Syenite
47659	N.D.	Karbøl junction		2.29	5.4	Bio-MPx
47660	N.D.	Karbøl junction		2.75	6.5	Carbonatite
47661	N.D.	Karbøl road		1.21	2.9	Globulite
47662	N.D.	Karbøl road		0.17	0.4	Syenite
47663	N.D.	Dalmoen		0.14	0.3	Syenite
47664	N.D.	Dalmoen		1.08	2.6	Globulite
47665	N.D.	Dalmoen		1.20	2.8	Globulite
47666	N.D.	Dalmoen		1.37	3.2	Globulite
47667	N.D.	Lake Skardvann		1.21	2.9	MPx

Appendix 2. Analytical values for P₂O₅ in weight % listed in order of decreasing values.

SAMPLE	4A P ₂ O ₅ %	4B P ₂ O ₅ %	4A+B P ₂ O ₅ %	CALC. % APATITE	LITHO. CODE
Alkaline rocks:					
SKM-06	6.63	N.A.	6.63	15.7	Bnd-FspBio-CPx
SKM-56	6.55	N.A.	6.55	15.5	Bio-CPx
SKM-02	N.A.	6.47	6.47	15.3	FspBio-CPx
SKM-33	6.46	N.A.	6.46	15.3	Bio-CPx
SKM-95	6.32	N.A.	6.32	15.0	FspBio-CPx
SKM-25	6.16	N.A.	6.16	14.6	Bio-CGb
SKM-60	5.93	N.A.	5.93	14.1	Bio-CPx
SKM-111	N.A.	5.92	5.92	14.0	Bio-CGb
SKM-51	5.58	N.A.	5.58	13.2	Fsp-Vnd-MPx
SKM-17	5.42	N.A.	5.42	12.8	Bio-CPx
38667	Brentliknubben1	N.A.	4.78	11.3	Bio-CPx
SKM-29	4.58	N.A.	4.58	10.9	FspBio-CPx
SKM-101	4.56	N.A.	4.56	10.8	FspBio-MPx
SKM-92	4.32	N.A.	4.32	10.2	Bio-CPx
SKM-52	4.11	N.A.	4.11	9.7	Bio-MPx
SKM-106	N.A.	4.01	4.01	9.5	FspBio-CPx
SKM-110	3.83	N.A.	3.83	9.1	Bio-CGb
SKM-41	3.77	N.A.	3.77	8.9	Bio-MPx
SKM-48	3.75	N.A.	3.75	8.9	Bio-CGb
SKM-104	3.74	N.A.	3.74	8.9	FspBio-MPx
38673	Brentliknubben7	N.A.	3.53	8.4	Bio-CPx
SKM-55	3.48	N.A.	3.48	8.2	MPx
SKM-50	3.36	N.A.	3.36	8.0	Fsp-Vnd-MPx
SKM-90	3.31	N.A.	3.31	7.8	FspBio-CPx
SKM-30	3.28	N.A.	3.28	7.8	Fsp-Vnd-MPx
SKM-40	3.20	N.A.	3.20	7.6	Bnd-FspBio-MPx
SKM-97	N.A.	2.94	2.94	7.0	Bio-MPx
47660	Karbøl junction	N.A.	2.75	6.5	Carbonatite
SKM-14	2.64	N.A.	2.64	6.3	Fsp-MPx
SKM-08	2.59	N.A.	2.59	6.1	Bio-MPx
SKM-112	N.A.	2.47	2.47	5.9	MPx
SKM-07	N.A.	2.41	2.41	5.7	Bio-CPx
SKM-69	2.38	N.A.	2.38	5.6	Bio-MPx
47656	Karbøl junction	N.A.	2.37	5.6	Bio-MPx
SKM-42	2.33	N.A.	2.33	5.5	FspBio-CPx
SKM-77	2.30	N.A.	2.30	5.5	FspBio-MPx
47659	Karbøl junction	N.A.	2.29	5.4	Bio-MPx
SKM-04	2.17	N.A.	2.17	5.1	Fsp-CPx
SKM-93	N.A.	2.06	2.06	4.9	MGb
SKM-39	2.06	N.A.	2.06	4.9	MPx

SAMPLE	4A P₂O₅ %	4B P₂O₅ %	4A+B P₂O₅ %	CALC. % APATITE	LITHO. CODE
SKM-26	N.A.	2.03	2.03	4.8	Bio-CGb
38670	Brentliknubben4	N.A.	1.98	4.7	FspBio-CPx
SKM-15	1.92	N.A.	1.92	4.6	Fsp-MPx
SKM-83	1.90	N.A.	1.90	4.5	Bio-MGb
SKM-81	1.89	N.A.	1.89	4.5	FspBio-CPx
SKM-10	1.74	N.A.	1.74	4.1	FspBio-CPx
SKM-01	1.73	N.A.	1.73	4.1	Bnd-Bio-CPx
SKM-35	1.71	N.A.	1.71	4.1	CPx
SKM-22	1.64	N.A.	1.64	3.9	Bnd-Bio-MGb
SKM-47	1.64	N.A.	1.64	3.9	MPx
SKM-13	1.64	N.A.	1.64	3.9	Fsp-Vnd-Bio-MPx
SKM-24	1.63	N.A.	1.63	3.9	MGb
SKM-11	1.61	N.A.	1.61	3.8	Bio-MPx
SKM-05	1.58	N.A.	1.58	3.7	Bio-MPx
SKM-94	1.51	N.A.	1.51	3.6	Fsp-MPx
SKM-89	1.51	N.A.	1.51	3.6	Fsp-Vnd-Bio-MPx
SKM-73	1.42	N.A.	1.42	3.4	Fsp-Vnd-Bio-MPx
SKM-58	N.A.	1.41	1.41	3.3	FspBio-CPx
47666	Dalmoen	N.A.	1.37	3.2	Globulite
SKM-12	1.33	N.A.	1.33	3.2	Fsp-Vnd-MPx
SKM-09	N.A.	1.32	1.32	3.1	MPx
SKM-99	1.29	N.A.	1.29	3.1	Bio-MPx
SKM-46	N.A.	1.27	1.27	3.0	Bio-MPx
SKM-109	1.27	N.A.	1.27	3.0	Globulite
SKM-16	1.23	N.A.	1.23	2.9	Fsp-MPx
SKM-108	1.22	N.A.	1.22	2.9	Fsp-Vnd-MPx
47667	Lake Skardvann	N.A.	1.21	2.9	MPx
47661	Dalmoen	N.A.	1.21	2.9	Globulite
47665	Dalmoen	N.A.	1.20	2.8	Globulite
SKM-79	1.17	N.A.	1.17	2.8	Fsp-Vnd-MPx
38676	Skardbakken2	N.A.	1.15	2.7	CarbBio-MPx
SKM-76	1.12	N.A.	1.12	2.7	Fsp-Vnd-Bio-MPx
SKM-65	N.A.	1.11	1.11	2.6	Bio-CPx
SKM-67	1.11	N.A.	1.11	2.6	Bio-MPx
SKM-96	1.09	N.A.	1.09	2.6	Bio-MPx
SKM-84	1.09	N.A.	1.09	2.6	Fsp-Vnd-Bio-MPx
SKM-74	1.08	N.A.	1.08	2.6	CGb
SKM-98	1.08	N.A.	1.08	2.6	Bio-CGb
47664	Dalmoen	N.A.	1.08	2.6	Globulite
SKM-88	1.04	N.A.	1.04	2.5	Bio-MPx
SKM-34	1.02	N.A.	1.02	2.4	Bio-CPx
SKM-37	0.98	N.A.	0.98	2.3	MPx
SKM-91	0.97	N.A.	0.97	2.3	Bio-MPx

SAMPLE	4A P₂O₅ %	4B P₂O₅ %	4A+B P₂O₅ %	CALC. % APATITE	LITHO. CODE
SKM-38	0.94	N.A.	0.94	2.2	Bnd-Bio-MPx
SKM-31	0.93	N.A.	0.93	2.2	Bio-MPx
SKM-44	N.A.	0.89	0.89	2.1	Bio-MPx
SKM-71	0.89	N.A.	0.89	2.1	Bio-MPx
SKM-19	0.88	N.A.	0.88	2.1	Bio-MGb
SKM-100	0.80	N.A.	0.80	1.9	FspBio-CPx
SKM-66	0.80	N.A.	0.80	1.9	Bio-MPx
SKM-32	N.A.	0.75	0.75	1.8	Bio-MPx
SKM-49	0.75	N.A.	0.75	1.8	Bio-MPx
SKM-80	0.68	N.A.	0.68	1.6	FspBio-CPx
38675	Skardbakken1	N.A.	0.68	1.6	FspBio-CPx
SKM-59	0.64	N.A.	0.64	1.5	Fsp-Vnd-Bio-MPx
47657	Karbøl junction	N.A.	0.53	1.3	Bio-MPx
SKM-18	N.A.	0.49	0.49	1.2	FspBio-MPx
SKM-75	0.46	N.A.	0.46	1.1	FspBio-MPx
SKM-57	0.43	N.A.	0.43	1.0	FspBio-MPx
38674	Nonshaugen	N.A.	0.41	1.0	Bio-MPx
SKM-86	0.39	N.A.	0.39	0.9	Fsp-Vnd-MPx
SKM-54	0.38	N.A.	0.38	0.9	Fsp-Vnd-MPx
SKM-53	0.35	N.A.	0.35	0.8	FspBio-MPx
SKM-61	0.32	N.A.	0.32	0.8	Bio-MPx
SKM-27	0.29	N.A.	0.29	0.7	Bio-MPx
SKM-68	N.A.	0.26	0.26	0.6	MPx
SKM-45	N.A.	0.24	0.24	0.6	Bio-CPx
SKM-70	N.A.	0.22	0.22	0.5	Bio-CGb
47658	Karbøl junction	N.A.	0.20	0.5	Syenite
47662	Karbøl road	N.A.	0.17	0.4	Syenite
47663	Dalmoen	N.A.	0.14	0.3	Syenite
SKM-03	N.A.	0.12	0.12	0.3	MGb
SKM-28	0.11	N.A.	0.11	0.3	Bio-CPx
SKM-20	0.10	N.A.	0.10	0.2	Fsp-CPx
SKM-87	0.09	N.A.	0.09	0.2	Fsp-Vnd-Bio-MPx
SKM-72	N.A.	0.07	0.07	0.2	Syenite
Wall rocks:					
SKM-82	0.89	N.A.	0.89	2.1	PxGranitoid
38669	Brentliknub.3	N.A.	0.70	1.7	Marble
SKM-63	0.66	N.A.	0.66	1.6	PxGranitoid
38671	Brentliknub.5	N.A.	0.43	1.0	Marble
SKM-62	0.32	N.A.	0.32	0.8	Granitoid
SKM-103	0.26	N.A.	0.26	0.6	Granitoid
SKM-85	0.21	N.A.	0.21	0.5	Marble
SKM-78	0.19	N.A.	0.19	0.5	Gneiss
SKM-64	0.18	N.A.	0.18	0.4	Marble

SAMPLE	4A P₂O₅ %	4B P₂O₅ %	4A+B P₂O₅ %	CALC. % APATITE	LITHO. CODE
SKM-23	0.17	N.A.	0.17	0.4	Marble
SKM-105	0.17	N.A.	0.17	0.4	Marble
SKM-107	0.10	N.A.	0.10	0.2	Gneiss
SKM-102	0.04	N.A.	0.04	0.1	Marble
38672	Brentliknub.6	N.A.	0.03	0.1	Soapstone
SKM-36	0.02	N.A.	0.02	0.0	Soapstone
SKM-21	0.02	N.A.	0.02	0.0	Marble
SKM-43	0.02	N.A.	0.02	0.0	Marble
38668	Brentliknub.2	N.A.	0.02	0.1	Marble

Appendix 3. Analytical values for P₂O₅ in weight % grouped according to lithological types and then listed in order of decreasing values.

SAMPLE	4A P ₂ O ₅ %	4B P ₂ O ₅ %	4A+B P ₂ O ₅ %	CALC. % APATITE	LITHO. CODE
Alkaline rocks:					
SKM-74	1.08	N.A.	1.08	2.6	CGb
SKM-25	6.16	N.A.	6.16	14.6	Bio-CGb
SKM-111	N.A.	5.92	5.92	14.0	Bio-CGb
SKM-110	3.83	N.A.	3.83	9.1	Bio-CGb
SKM-48	3.75	N.A.	3.75	8.9	Bio-CGb
SKM-26	N.A.	2.03	2.03	4.8	Bio-CGb
SKM-98	1.08	N.A.	1.08	2.6	Bio-CGb
SKM-70	N.A.	0.22	0.22	0.5	Bio-CGb
SKM-93	N.A.	2.06	2.06	4.9	MGb
SKM-24	1.63	N.A.	1.63	3.9	MGb
SKM-03	N.A.	0.12	0.12	0.3	MGb
SKM-83	1.90	N.A.	1.90	4.5	Bio-MGb
SKM-19	0.88	N.A.	0.88	2.1	Bio-MGb
SKM-22	1.64	N.A.	1.64	3.9	Bnd-Bio-MGb
SKM-35	1.71	N.A.	1.71	4.1	CPx
SKM-56	6.55	N.A.	6.55	15.5	Bio-CPx
SKM-33	6.46	N.A.	6.46	15.3	Bio-CPx
SKM-60	5.93	N.A.	5.93	14.1	Bio-CPx
SKM-17	5.42	N.A.	5.42	12.8	Bio-CPx
38667	Brentliknub.1	N.A.	4.78	11.3	Bio-CPx
SKM-92	4.32	N.A.	4.32	10.2	Bio-CPx
38673	Brentliknub.7	N.A.	3.53	8.4	Bio-CPx
SKM-07	N.A.	2.41	2.41	5.7	Bio-CPx
SKM-65	N.A.	1.11	1.11	2.6	Bio-CPx
SKM-34	1.02	N.A.	1.02	2.4	Bio-CPx
SKM-45	N.A.	0.24	0.24	0.6	Bio-CPx
SKM-28	0.11	N.A.	0.11	0.3	Bio-CPx
SKM-04	2.17	N.A.	2.17	5.1	Fsp-CPx
SKM-20	0.10	N.A.	0.10	0.2	Fsp-CPx
SKM-02	N.A.	6.47	6.47	15.3	FspBio-CPx
SKM-95	6.32	N.A.	6.32	15.0	FspBio-CPx
SKM-29	4.58	N.A.	4.58	10.9	FspBio-CPx
SKM-106	N.A.	4.01	4.01	9.5	FspBio-CPx
SKM-90	3.31	N.A.	3.31	7.8	FspBio-CPx
SKM-42	2.33	N.A.	2.33	5.5	FspBio-CPx
38670	Brentliknub.4	N.A.	1.98	4.7	FspBio-CPx
SKM-81	1.89	N.A.	1.89	4.5	FspBio-CPx
SKM-10	1.74	N.A.	1.74	4.1	FspBio-CPx
SKM-58	N.A.	1.41	1.41	3.3	FspBio-CPx

SAMPLE	4A P ₂ O ₅ %	4B P ₂ O ₅ %	4A+B P ₂ O ₅ %	CALC. % APATITE	LITHO. CODE
SKM-100	0.80	N.A.	0.80	1.9	FspBio-CPx
SKM-80	0.68	N.A.	0.68	1.6	FspBio-CPx
38675	Skardbakken1	N.A.	0.68	1.6	FspBio-CPx
SKM-01	1.73	N.A.	1.73	4.1	Bnd-Bio-CPx
SKM-06	6.63	N.A.	6.63	15.7	Bnd-FspBio-CPx
SKM-55	3.48	N.A.	3.48	8.2	MPx
SKM-112	N.A.	2.47	2.47	5.9	MPx
SKM-39	2.06	N.A.	2.06	4.9	MPx
SKM-47	1.64	N.A.	1.64	3.9	MPx
SKM-09	N.A.	1.32	1.32	3.1	MPx
47667	Lake Skardvann	N.A.	1.21	2.9	MPx
SKM-37	0.98	N.A.	0.98	2.3	MPx
SKM-68	N.A.	0.26	0.26	0.6	MPx
SKM-52	4.11	N.A.	4.11	9.7	Bio-MPx
SKM-41	3.77	N.A.	3.77	8.9	Bio-MPx
SKM-97	N.A.	2.94	2.94	7.0	Bio-MPx
SKM-08	2.59	N.A.	2.59	6.1	Bio-MPx
SKM-69	2.38	N.A.	2.38	5.6	Bio-MPx
47656	Karbøl junction	N.A.	2.37	5.6	Bio-MPx
47659	Karbøl junction	N.A.	2.29	5.4	Bio-MPx
SKM-11	1.61	N.A.	1.61	3.8	Bio-MPx
SKM-05	1.58	N.A.	1.58	3.7	Bio-MPx
SKM-99	1.29	N.A.	1.29	3.1	Bio-MPx
SKM-46	N.A.	1.27	1.27	3.0	Bio-MPx
SKM-67	1.11	N.A.	1.11	2.6	Bio-MPx
SKM-96	1.09	N.A.	1.09	2.6	Bio-MPx
SKM-88	1.04	N.A.	1.04	2.5	Bio-MPx
SKM-91	0.97	N.A.	0.97	2.3	Bio-MPx
SKM-31	0.93	N.A.	0.93	2.2	Bio-MPx
SKM-44	N.A.	0.89	0.89	2.1	Bio-MPx
SKM-71	0.89	N.A.	0.89	2.1	Bio-MPx
SKM-66	0.80	N.A.	0.80	1.9	Bio-MPx
SKM-32	N.A.	0.75	0.75	1.8	Bio-MPx
SKM-49	0.75	N.A.	0.75	1.8	Bio-MPx
47657	Karbøl junction	N.A.	0.53	1.3	Bio-MPx
38674	Nonshaugen	N.A.	0.41	1.0	Bio-MPx
SKM-61	0.32	N.A.	0.32	0.8	Bio-MPx
SKM-27	0.29	N.A.	0.29	0.7	Bio-MPx
38676	Skardbakken2	N.A.	1.15	2.7	CarbBio-MPx
SKM-14	2.64	N.A.	2.64	6.3	Fsp-MPx
SKM-15	1.92	N.A.	1.92	4.6	Fsp-MPx
SKM-94	1.51	N.A.	1.51	3.6	Fsp-MPx
SKM-16	1.23	N.A.	1.23	2.9	Fsp-MPx

SAMPLE	4A P ₂ O ₅ %	4B P ₂ O ₅ %	4A+B P ₂ O ₅ %	CALC. % APATITE	LITHO. CODE
SKM-101	4.56	N.A.	4.56	10.8	FspBio-MPx
SKM-104	3.74	N.A.	3.74	8.9	FspBio-MPx
SKM-77	2.30	N.A.	2.30	5.5	FspBio-MPx
SKM-18	N.A.	0.49	0.49	1.2	FspBio-MPx
SKM-75	0.46	N.A.	0.46	1.1	FspBio-MPx
SKM-57	0.43	N.A.	0.43	1.0	FspBio-MPx
SKM-53	0.35	N.A.	0.35	0.8	FspBio-MPx
SKM-51	5.58	N.A.	5.58	13.2	Fsp-Vnd-MPx
SKM-50	3.36	N.A.	3.36	8.0	Fsp-Vnd-MPx
SKM-30	3.28	N.A.	3.28	7.8	Fsp-Vnd-MPx
SKM-12	1.33	N.A.	1.33	3.2	Fsp-Vnd-MPx
SKM-108	1.22	N.A.	1.22	2.9	Fsp-Vnd-MPx
SKM-79	1.17	N.A.	1.17	2.8	Fsp-Vnd-MPx
SKM-86	0.39	N.A.	0.39	0.9	Fsp-Vnd-MPx
SKM-54	0.38	N.A.	0.38	0.9	Fsp-Vnd-MPx
SKM-13	1.64	N.A.	1.64	3.9	Fsp-Vnd-Bio-MPx
SKM-89	1.51	N.A.	1.51	3.6	Fsp-Vnd-Bio-MPx
SKM-73	1.42	N.A.	1.42	3.4	Fsp-Vnd-Bio-MPx
SKM-76	1.12	N.A.	1.12	2.7	Fsp-Vnd-Bio-MPx
SKM-84	1.09	N.A.	1.09	2.6	Fsp-Vnd-Bio-MPx
SKM-59	0.64	N.A.	0.64	1.5	Fsp-Vnd-Bio-MPx
SKM-87	0.09	N.A.	0.09	0.2	Fsp-Vnd-Bio-MPx
SKM-38	0.94	N.A.	0.94	2.2	Bnd-Bio-MPx
SKM-40	3.20	N.A.	3.20	7.6	Bnd-FspBio-MPx
47660	Karbøl junction	N.A.	2.75	6.5	Carbonatite
47658	Karbøl junction	N.A.	0.20	0.5	Syenite
47662	Karbøl road	N.A.	0.17	0.4	Syenite
47663	Dalmoen	N.A.	0.14	0.3	Syenite
SKM-72	N.A.	0.07	0.07	0.2	Syenite
47666	Dalmoen	N.A.	1.37	3.2	Globulite
SKM-109	1.27	N.A.	1.27	3.0	Globulite
47661	Dalmoen	N.A.	1.21	2.9	Globulite
47665	Dalmoen	N.A.	1.20	2.8	Globulite
47664	Dalmoen	N.A.	1.08	2.6	Globulite
Wall rocks:					
SKM-62	0.32	N.A.	0.32	0.8	Granitoid
SKM-103	0.26	N.A.	0.26	0.6	Granitoid
SKM-82	0.89	N.A.	0.89	2.1	PxGranitoid
SKM-63	0.66	N.A.	0.66	1.6	PxGranitoid
38672	Brentliknub.6	N.A.	0.03	0.1	Soapstone
SKM-36	0.02	N.A.	0.02	0.0	Soapstone
SKM-78	0.19	N.A.	0.19	0.5	Gneiss

SAMPLE	4A P ₂ O ₅ %	4B P ₂ O ₅ %	4A+B P ₂ O ₅ %	CALC. % APATITE	LITHO. CODE
SKM-107	0.10	N.A.	0.10	0.2	Gneiss
38669	Brentliknub.3	N.A.	0.70	1.7	Marble
38671	Brentliknub.5	N.A.	0.43	1.0	Marble
SKM-85	0.21	N.A.	0.21	0.5	Marble
SKM-64	0.18	N.A.	0.18	0.4	Marble
SKM-23	0.17	N.A.	0.17	0.4	Marble
SKM-105	0.17	N.A.	0.17	0.4	Marble
SKM-102	0.04	N.A.	0.04	0.1	Marble
SKM-21	0.02	N.A.	0.02	0.0	Marble
SKM-43	0.02	N.A.	0.02	0.0	Marble
38668	Brentliknub.2	N.A.	0.02	0.0	Marble

Appendix 4. Sample list showing the coordinates of the sampling points and petrographic description of the collected samples together with their lithological code shown in Appendix 5.

SAMPLE NUMBER	UTM		SAMPLE DESCRIPTION	LITHO. CODE
	Zone 33 W			
	East	North		
PRØVER 2008: MISVÆRDAL				
SKM-01	499505	7442340	Coarse-grained biotite-rich bands in mgr. green pyroxenite.	Bnd-Bio-CPx
SKM-02	499680	7442450	Cgr. biotite-rich dark green feldspathic pyroxenite with 5-10 mm black biotite laths as interstitial aggregates.	FspBio-CPx
SKM-03	499900	7442765	Mgr. gabbro with 1-3 mm hornblende needles intergrown with 1-5 mm light grey rectangular feldspar.	MGb
SKM-04	500045	7443355	Cgr. pyroxenite (5-10 mm) with some intergranular feldspar infiltration.	Fsp-CPx
SKM-05	499181	7442112	Mgr. green pyroxenite with variable cgr. biotite as dissemination, veins and segregations.	Bio-MPx
SKM-06	499837	7441955	Cgr. biotite-rich pyroxenite bands with some feldspar infiltration in mgr. biotite-altered pyroxenites.	Bnd-FspBio-CPx
SKM-07	498976	7441690	Cgr. biotite-rich pyroxenite with 3-5 mm biotite and 3-10 mm pyroxene.	Bio-CPx
SKM-08	498983	7441394	Mgr. biotite alteration with remnants of mgr. pyroxenite.	Bio-MPx
SKM-09	499010	7441028	Mgr. massive pyroxenite with scattered px. porphyries (5 mm) and minor interst. biotite.	MPx
SKM-10	499124	7441084	Cgr. biotite-rich feldspathic pyroxenite with up to 20 mm crystals of pyroxene and biotite.	FspBio-CPx
SKM-11	499225	7440615	Mgr. biotite-rich pyroxenite. Zone in MPx with minor biotite.	Bio-MPx
SKM-12	499035	7440829	Mgr. green massive pyroxenite containing some hairline feldspar veins.	Fsp-Vnd-MPx
SKM-13	498760	7440850	Mgr. pyroxenite with zones rich in biotite and/or 1 cm hbl. crystals. Some fsp. veins and infiltration.	Fsp-Vnd-Bio-MPx
SKM-14	498713	7440676	Mgr. pyroxenite with scattered crystals and aggregates of 1 cm pyroxene. Some infiltration of fsp (3 %).	Fsp-MPx
SKM-15	498973	7440609	Mgr. pyroxenite with irregular infiltration of subordinate feldspar.	Fsp-MPx
SKM-16	499112	7440379	Mgr. massive green pyroxenite containing minor infiltration of feldspar.	Fsp-MPx
SKM-17	499253	7440076	Cgr. (3-5 mm) gabbro with c. 10 % biotite.	Bio-CPx
SKM-18	501250	7442610	Mgr. pale green pyroxenite with 5 mm porphyries of feldspar, pyroxene and biotite.	FspBio-MPx
SKM-19	501292	7442236	Mgr. biotite-rich gabbro with 2-5 mm subsircular feldspar in a biotite-foliated matrix.	Bio-MGb
SKM-20	500991	7442061	Cgr. (3-5 mm) dark greenish pyroxenite infiltrated by feldspar aggregates. Sparse diss. of pyrite.	Fsp-CPx
SKM-21	501016	7442061	Mgr. (1-2 mm) pink and light green massive carbonate rock from 1 m thick zone.	Carbonate
SKM-22	501264	7442116	Mgr. biotite-bearing gabbro with bands rich in 2-7 mm spherical fsp., 10-20 mm pyroxene and 1-2 mm fsp.	Bnd-Bio-MGb

SAMPLE NUMBER	UTM Zone 33 W		SAMPLE DESCRIPTION	LITHO. CODE
	East	North		
SKM-23	501523	7442000	Fgr.-mgr. (0.5-2 mm) carbonate rock banded in shades of grey.	Carbonate
SKM-24	501638	7442135	Mgr. (2-3 mm) dark grey gabbro.	MGb
SKM-25	500226	7443475	Cgr. (5 mm) biotite gabbro with up to 8 mm biotite books.	Bio-CGb
SKM-26	500280	7443350	Cgr. gabbro with 2-10 mm pyroxene intergrown with 5-10 mm biotite partly as aggregates.	Bio-CGb
SKM-27	500780	7442796	Mgr. pale green pyroxenite with scattered lathes (1-3 mm), veinlets and small segregations of black biotite.	Bio-MPx
SKM-28	501047	7442871	Cgr. (5-8 mm) biotite-rich pyroxenite.	Bio-CPx
SKM-29	500510	7442850	Cgr. (5-10 mm) greyish green pyroxenite with interstitial coarse feldspar and subordinate biotite.	FspBio-CPx
SKM-30	499917	7441185	Mgr. pyroxenite with 1-20 mm wide fsp. veins rimmed by irregular infiltration of fsp. and coarse hbl. (5-7 mm) .	Fsp-Vnd-MPx
SKM-31	501030	7441625	Mgr. (1-2 mm) dark grey biotite-pyroxenite with minor feldspar.	Bio-MPx
SKM-32	500739	7441620	Mgr. dark greyish pyroxenite with densely spaced and weakly oriented black biotite (5 mm).	Bio-MPx
SKM-33	500746	7441830	Cgr. pyroxenite with 5-7 mm pale green pyroxene intergrown with abundant 5-10 mm biotite.	Bio-CPx
SKM-34	501004	7441849	Mgr. (2-3 mm) biotite-bearing dark greyish green pyroxenite.	Bio-CPx
SKM-35	501250	7441854	Cgr. (2-5 mm) dark grey to black pyroxenite/hornblende?	CPx
SKM-36	501227	7441599	Finely banded (1-2 cm) light green talc-rich soapstone with brown weathered carbonate-rich bands.	Soapstone
SKM-37	500753	7441382	Mgr. (1-3 mm) dark green pyroxenite.	MPx
SKM-38	499686	7442327	Mgr. (1-3 mm) dark grey pyroxenite with dm. bands enriched in biotite, hornblende and/or coarse pyroxene.	Bnd-Bio-MPx
SKM-39	500017	7442356	Mgr. (<1-2 mm) dark grey to black hornblende pyroxenite.	MPx
SKM-40	500072	7442604	Mgr. (1 mm) dark grey pyroxenite with alternating bands of more px.-, bio.- (3 mm) and fsp.-rich types.	Bnd-FspBio-MPx
SKM-41	500259	7442618	Mgr. green pyroxenite with irregularly distributed phenocrysts (5-10 mm) of biotite and hornblende.	Bio-MPx
SKM-42	500286	7442620	Cgr. pyroxenite with 5-10 mm pyroxene, 10-30 mm biotite and some interstitial feldspar.	FspBio-CPx
SKM-43	500294	7442371	Mgr. white carbonate rock as 2-5 cm bands separated by calc-silicate rocks.	Carbonate
SKM-44	499465	7442104	Mgr. pale green pyroxenite with abundant nearly monominerallic biotite aggregates.	Bio-MPx
SKM-45	499472	7441848	Cgr. (5-15 mm) biotite-rich pyroxenite with some feldspar infiltration.	Bio-CPx
SKM-46	499464	7441599	Mgr. (1-2 mm) dark grey biotite-rich pyroxenite.	Bio-MPx
SKM-47	499345	7441336	Mgr. dark green pyroxenite with mm wide pale green actinolite veins.	MPx

SAMPLE NUMBER	UTM		SAMPLE DESCRIPTION	LITHO. CODE
	Zone 33 W			
	East	North		
SKM-48	499297	7441171	Cgr. (3-8 mm) biotite gabbro.	Bio-CGb
SKM-49	499496	7441006	Mgr. greyish green pyroxenite with black biotite-hornblende lenses (1-5 mm x 20-50 mm).	Bio-MPx
SKM-50	499227	7440773	Mgr. green pyroxenite with parallel veins of coarse hornblende (1 cm) and/or feldspar.	Fsp-Vnd-MPx
SKM-51	499762	7441480	Mgr. (1-2 mm) dark grey hornblende pyroxenite with network of fsp.-hbl. veins and infiltration.	Fsp-Vnd-MPx
SKM-52	499724	7441613	Mgr. (1-2 mm) pyroxenite with laths (5 mm) and large aggregates of biotite.	Bio-MPx
SKM-53	499683	7441820	Mgr. (1-3 mm) pale green pyroxenite with actinolite-filled fractures, some bio. and fsp. aggregates	FspBio-MPx
SKM-54	499733	7442107	Mgr. (1-2 mm) dark grey biotite-bearing pyroxenite with thin fsp. veins rimmed by actinolite infiltration .	Fsp-Vnd-MPx
SKM-55	498719	7441769	Mgr. dark green pyroxenite with minor feldspar veinlets.	MPx
SKM-56	498825	7441582	Cgr. (2-8 mm) pale green fsp. pyroxenite with actinolite-coated fractures and some biotite aggregates.	Bio-CPx
SKM-57	498745	7441099	Mgr. (1-2 mm) pale green pyroxenite with 5-10 mm feldspar porphyries and scattered biotite aggr.	FspBio-MPx
SKM-58	498647	7440952	Cgr. (3-10 mm) biotite-rich pyroxenite with some feldspar infiltration.	FspBio-CPx
SKM-59	498557	7441226	Mgr. (2-3 mm) pale green pyroxenite with scattered feldspar veins along foliation defined by biotite.	Fsp-Vnd-Bio-MPx
SKM-60	498542	7441473	Cgr. (5-20 mm) pale green pyroxenite containing black bands of coarse biotite (5-10 mm).	Bio-CPx
SKM-61	499768	7441461	Mgr. (2-3 mm) pale green pyroxenite with diss. biotite crystals (1-5 mm) and actinolite fractures.	Bio-MPx
SKM-62	501077	7440637	Mgr. (2-3 mm) grey hornblende-bearing quartz diorite.	Granitoid
SKM-63	500995	7440360	Cgr. (2-5 mm) grey diorite with small inclusions of mgr. pyroxenite.	PxGranitoid
SKM-64	501203	7440508	Fine-grained (fgr.) light grey and grey banded carbonate rock.	Carbonate
SKM-65	501439	7441885	Cgr. (2-5 mm) green pyroxenite with disseminated biotite.	Bio-CPx
SKM-66	501768	7441847	Mgr. dark greenish pyroxenite lenses (5 cm) in matrix av mgr. pale green pyroxenite, both with bio. diss.	Bio-MPx
SKM-67	501404	7441597	Mgr. (1-3 mm) pale green pyroxenite with dense dissemination of coarse biotite crystals.	Bio-MPx
SKM-68	501275	7441379	Mgr. pale green massive pyroxenite.	MPx
SKM-69	501036	7441320	Mgr. (2-4 mm) dark green to black biotite-rich pyroxenite.	Bio-MPx
SKM-70	501798	7441372	Cgr. (5 mm) biotite-rich gabbro with 15-20 % white feldspar.	Bio-CGb
SKM-71	501886	7441391	Mgr. pale green pyroxenite with disseminated biotite (1-2 mm).	Bio-MPx
SKM-72	499010	7441028	Cgr. syenite composed of pale bluish grey fsp. (5-30 mm), hbl. crystals (5-10 mm) and titanite (3-5 mm).	Syenite

SAMPLE NUMBER	UTM		SAMPLE DESCRIPTION	LITHO. CODE
	Zone 33 W			
	East	North		
SKM-73	501751	7441153	Mgr.-cgr. pale green pyroxenite with diss. bio. (1-5 mm), fsp. cryst. , fsp. veins and dark green fgr. lenses.	Fsp-Vnd-Bio-MPx
SKM-74	501555	7440903	Cgr. (3-5 mm) gabbro with pale pinkish feldspar. Rusty and crumbles easily.	CGb
SKM-75	501197	7440872	Mgr. (1-2 mm) pale green schistose pyroxenite with diss. biotite (2-5 mm) and minor coarse fsp. cryst.	FspBio-MPx
SKM-76	501243	7440637	Mgr. (1-2 mm) pale green sheared pyroxenite with diss. biotite (1-10 mm) and some fsp.-hbl. veins.	Fsp-Vnd-Bio-MPx
SKM-77	501774	7440388	Mgr. pale green foliated pyroxenite with abundant 3-15 mm bio. lathes and some fsp. augens.	FspBio-MPx
SKM-78	501762	7440560	Alternating cgr. and fgr. light grey feldspathic bands with scattered 5-10 mm bio. flakes and rusty patches.	Gneiss
SKM-79	501556	7440603	Mgr. pale green pyroxenite with feldspar-hornblende aggregates assoc. with 2-10 mm fsp.-hbl. veins	Fsp-Vnd-MPx
SKM-80	500968	7441058	Cgr. (2-5 mm) dark green biotite pyroxenite with some feldspar infiltration.	FspBio-CPx
SKM-81	500761	7440377	Cgr. (2-5 mm) pyroxenite with some bio. (2-3 mm) and infiltration of feldspar-hbl. aggregates.	FspBio-CPx
SKM-82	500780	7440095	Cgr. (2-5 mm) bio. diorite with small feldspar porphyritic pyroxenite inclusions cut by white fsp. veins.	PxGranitoid
SKM-83	500558	7440318	Grey medium-grained (1-3 mm) gabbro with some disseminated biotite (1-2 mm).	Bio-MGb
SKM-84	500503	7440134	Mgr. pale green pyroxenite with scattered bio. lathes (1-5 mm) and fsp.-hbl. veins and infiltration.	Fsp-Vnd-Bio-MPx
SKM-85	500485	7440103	Fine-grained light grey, bluish grey and white banded carbonate rock	Carbonate
SKM-86	500211	7440265	Mgr. pale green pyroxenite with scattered 1-2 mm wide feldspar veins.	Fsp-Vnd-MPx
SKM-87	500800	7441114	Mgr. schistose dark grey biotite-rich pyroxenite with scattered 2 mm wide feldspar veins and grains.	Fsp-Vnd-Bio-MPx
SKM-88	500516	7441367	Mgr. (2-3 mm) dark green biotite-rich pyroxenite with cgr. hornblende (1-3 cm) segregations.	Bio-MPx
SKM-89	500614	7441581	Mgr. dark green pyroxenite with cm thick bio.-rich bands, and fsp.-hbl. veins and infiltration.	Fsp-Vnd-Bio-MPx
SKM-90	500466	7440998	Cgr. (3-10 mm) dark grey pyroxenite with abundant biotite (<10 mm) and some fsp. (5-10 mm) infiltration	FspBio-CPx
SKM-91	500276	7441357	Mgr. (1-3 mm) dark green bio.-bearing pyroxenite with biotite-rich zones.	Bio-MPx
SKM-92	500251	7441684	Cgr. (2-5 mm) dark greenish black pyroxenite with minor biotite and hornblende.	Bio-CPx
SKM-93	499939	7441601	Mgr. grey pyroxene porphyritic (3-8 mm) gabbro.	MGb
SKM-94	500084	7441303	Mgr. (1-2 mm) dark greyish green pyroxenite with patchy infiltration of feldspar (30-40 %).	Fsp-MPx
SKM-95	500339	7441101	Cgr. (2-5 mm) biotite pyroxenite with some 5 mm feldspar grains.	FspBio-CPx
SKM-96	500393	7442539	Mgr. (2-3 mm) dark grey foliated biotite-rich pyroxenite.	Bio-MPx
SKM-97	500877	7442568	Mgr. (1-2 mm) dark grey biotite-rich pyroxenite.	Bio-MPx

SAMPLE NUMBER	UTM Zone 33 W		SAMPLE DESCRIPTION	LITHO. CODE
	East	North		
SKM-98	500554	7442183	Cgr. (2-8 mm) biotite gabbro with pale green pyroxene and black biotite.	Bio-CGb
SKM-99	500644	7442045	Mgr. (1-5 mm) dark grey pyroxenite with black biotite-rich schlieren.	Bio-MPx
SKM-100	500353	7441853	Cgr. (5-20 mm) biotite-rich pyroxenite with minor fsp. infiltration and up to 30 mm biotite crystals.	FspBio-CPx
SKM-101	500031	7442037	Mgr. (1-3 mm) dark grey feldspathic pyroxenite with scattered 2-5 mm biotite crystals and aggregates.	FspBio-MPx
SKM-102	500382	7440873	Mgr. (1-2 mm) light yellowish to reddish brown carbonate rock.	Carbonate
SKM-103	500247	7440872	Grey coarse-grained (5 mm) biotite-bearing granodiorite with feldspar veinlets.	Granitoid
SKM-104	500033	7440825	Mgr. (1-3 mm) dark green foliated pyroxenite with 3-5 mm bio. aggr. and 1-2 cm feldspar-rich zones.	FspBio-MPx
SKM-105	500740	7442350	Fine-grained greyish white carbonate rock with parallel silicate laminae (<1 mm).	Carbonate
SKM-106	500697	7442313	Cgr. (3-10 mm) dark green pyroxenite with some biotite and feldspar infiltration.	FspBio-CPx
SKM-107	499637	7439527	Mgr. (1-2 mm) dark grey banded biotite gneiss with alternating feldspar- and biotite-rich bands.	Gneiss
SKM-108	500157	7443169	Mgr. green massive pyroxenite with some 1-5 mm thick feldspar veins.	Fsp-Vnd-MPx
SKM-109	499605	7439532	Mgr. (1-2 mm) feldspar-rich elliptical globules separated by 2-5 mm wide mafic zones.	Globulite
SKM-110	499732	7442467	Cgr. (5-10 mm) biotite gabbro with 2-3 cm thick fine-grained pale green folded zones.	Bio-CGb
SKM-111	500420	7442825	Cgr. (5-10 mm) biotite gabbro with irregularly distributed interstitial feldspar.	Bio-CGb
SKM-112	499200	7442187	Fgr. green pyroxenite with 5-10 mm phenocrysts of black pyroxene from 30 cm dyke.	MPx
PRØVER 2008: HOPSFJELLET				
HF-01	487171	7565136	Medium- to coarse-grained grey talc-serpentinite-anthophyllite schist with banded enrichments of talc.	Mg-rich schist
HF-02	487424	7465314	Fine- to medium-grained grey talc-bearing schist with 5-20 mm thick dark grey biotite-rich bands.	Mg-rich schist
HF-03	487783	7465456	Fine- to medium-grained light grey talc-chlorite schist with 1-5 mm light grey talcaceous bands.	Mg-rich schist
HF-04	488207	7466298	Fine- to medium-grained grey chlorite-rich talc-rich schist.	Mg-rich schist
HF-05	488048	7465863	Fine- to medium-grained light grey talc-chlorite schist with thin talc-rich lenses.	Mg-rich schist
PRØVER 2007: MISVÆRDAL				
38667	500170	7442720	Cgr. biotite pyroxenite.	Bio-CPx
38668	500170	7442720	Green banded light grey carbonate rock	Carbonate

SAMPLE NUMBER	UTM Zone 33 W		SAMPLE DESCRIPTION	LITHO. CODE
	East	North		
38669	500170	7442720	Dark grey biotite-rich carbonate rock	Carbonate
38670	500170	7442720	Cgr. biotite pyroxenite with coarse-grained feldspar infiltration.	FspBio-CPx
38671	500170	7442720	Light grey thin-banded carbonate rock	Carbonate
38672	500170	7442720	Fgr. talc-rich rock	Soapstone
38673	500420	7442825	Cgr. biotite gabbro with irregularly distributed interstitial feldspar.	Bio-CPx
38674	499920	7442710	Mgr. dark foliated biotite gabbro with white feldspar augens.	Bio-MPx
38675	499440	7441775	Cgr. biotite pyroxenite with infiltration of feldspar aggregates.	FspBio-CPx
38676	499440	7441775	Grey biotite-carbonate zone in mgr. pyroxenite with faint biotite foliation.	CarbBio-MPx
PRØVER 2006: MISVÆRDAL				
47656	499455	7442300	Mgr. weakly foliated biotite-altered pyroxenite with minor pyrite and accessory chalcopyrite	Bio-MPx
47657	499455	7442300	Mgr. strongly biotite altered sandy pyroxenite.	Bio-MPx
47658	499455	7442300	Cgr. grey syenite with brownish ?titanite prisms.	Syenite
47659	499455	7442300	Mgr. strongly biotite altered pyroxenite	Bio-MPx
47660	499455	7442300	Cgr. light pinkish grey carbonate rock with coarse hornblende crystals in a dyke.	Carbonatite
47661	499176	7442038	Cgr. light greyish hornblende-biotite syenite with brownish ?titanite needles.	Syenite
47662	499176	7442038	Cgr. grey biotite-hornblende syenite	Syenite
47663	499595	7439545	Mgr. pinkish syenite with leucocratic veinlets and hornblende patches.	Syenite
47664	499595	7439545	Mgr. felsic globules rimmed by 2-8 mm mafic aggregates.	Globulite
47665	499595	7439545	Mgr. weakly foliated felsic globulite.	Globulite
47666	499595	7439545	Part of globulite consisting of 5-10 mm grey feldspar lathes in hornblende dominated matrix.	Globulite
47667	499485	7441000	Mgr. grey pyroxenite with minor biotite.	MPx

Appendix 5. Table showing the different abbreviations or lithological codes for the sampled rocks shown in Appendix 1-4 together with transformation factors used in the calculation of apatite contents and grain-size terminology used in the text.

LITHOLOGICAL CODE	SAMPLED ROCK
Bio-CGb	Coarse-grained biotite gabbro
Bio-CPx	Coarse-grained biotite pyroxenite
Bio-MGb	Medium-grained biotite gabbro
Bio-MPx	Medium-grained biotite pyroxenite
Bnd-Bio-CPx	Bands of coarse-grained biotite pyroxenite
Bnd-Bio-MGb	Bands of medium-grained biotite gabbro
Bnd-Bio-MPx	Bands of medium-grained biotite pyroxenite
Bnd-FspBio-CPx	Bands of coarse-grained feldspathic biotite pyroxenite
Bnd-FspBio-MPx	Bands of medium-grained feldspathic biotite pyroxenite
CarbBio-MPx	Medium-grained carbonate-rich biotite pyroxenite
Carbonate	Sedimentary carbonate, low in Sr.
Carbonatite	Magmatic carbonate, high in Sr.
CGb	Coarse-grained gabbro
CPx	Coarse-grained pyroxenite
FspBio-CPx	Coarse-grained feldspathic biotite pyroxenite
FspBio-MPx	Medium-grained feldspathic biotite pyroxenite
Fsp-CPx	Coarse-grained feldspathic pyroxenite
Fsp-MPx	Medium-grained feldspathic pyroxenite
Fsp-Vnd-Bio-MPx	Feldspar-veined medium-grained biotite pyroxenite
Fsp-Vnd-MPx	Feldspar-veined medium-grained pyroxenite
Globulite	Felsic orbicular rock, i.e. felsic globules in mafic matrix
Gneiss	Micaceous quartz-feldspathic gneiss
Granitoid	Coarse-grained quartz diorite and granodiorite
Marble	Sedimentary carbonate, low in Sr.
MGb	Medium-grained gabbro
Mg-rich schist	Talc-serpentine-chlorite schist
MPx	Medium-grained pyroxenite
PxGranitoid	Granitoids with small inclusions of medium-grained pyroxenite
Soapstone	Ultramafic talc-serpentine-carbonate rock
Syenite	Coarse-grained pink to bluish grey alkali-feldspar syenite

$P_{2.29} = P_{2O_5}$

$P_{5.43} = \text{Weight \% apatite}$

$P_{2O_5}_{2.37} = \text{Weight \% fluor-apatite}$

Fine-grained = < 1 mm

Medium-grained = 1-3 mm

Coarse-grained = 3-10 mm

Very coarse-grained = 10-30 mm

Pegmatitic = > 30 mm



Norges geologiske undersøkelse
Postboks 6315, Sluppen
7491 Trondheim, Norge

Besøksadresse
Leiv Eirikssons vei 39, 7040 Trondheim

Telefon 73 90 40 00
Telefax 73 92 16 20
E-post ngu@ngu.no
Nettside www.ngu.no

*Geological Survey of Norway
PO Box 6315, Sluppen
7491 Trondheim, Norway*

*Visitor address
Leiv Eirikssons vei 39, 7040 Trondheim*

*Tel (+ 47) 73 90 40 00
Fax (+ 47) 73 92 16 20
E-mail ngu@ngu.no
Web www.ngu.no/en-gb/*